Figure 4 Upper panel: Ouabain-induced dialysate noradrenaline (NA) release in various Ca^{2+} interventions. Total NA release evoked by ouabain was suppressed by the pretreatment with ω-conotoxin GVIA, verapamil, TMB-8. Lower panel: Ouabain-induced dialysate acetylcholine (ACh) release in various Ca^{2+} interventions. Total ACh release evoked by ouabain was suppressed by the pretreatment with ω-conotoxin MVIICA or TMB-8. Values are presented as the mean ± SE (for each column $n = 6$). *$P < 0.05$ vs. vehicle.

affected ACh release but ω-conotoxin MVIIC inhibited ACh release evoked by ouabain. Furthermore, KB-7943 did not affect either the ACh release evoked by ouabain. These data suggest that N or L-type Ca^{2+} channels or reversal Na^+/Ca^{2+} exchange might not be responsible for the ACh release evoked by ouabain. However, a marked suppression of ouabain-induced ACh release was observed with the addition of P/Q types channel blocker or TMB-8. In the case of parasympathetic nerve endings, Ca^{2+} elevation coupled to ACh release might be derived via internal stores or Ca^{2+} channels (P/Q types) rather than Na^+/Ca^{2+} exchange (Casali et al. 1995, Kawada et al. (in press)).

In the case of NA, ω-conotoxin GVIA or verapamil suppressed the NA release evoked by ouabain. Ouabain-induced NA release was independent of depolarization (TTX-resistant) but associated with the opening of Ca^{2+} channel. Furthermore, neither KB-7493 nor dichlorobenzamil affected the NA release evoked by ouabain. These data suggest that bi-directions of

Na^+/Ca^{2+} exchange might not be responsible for the elevation of intracellular Ca^{2+} levels evoked by ouabain. A marked suppression of ouabain-induced NA release was observed with the addition of TMB-8. Taking these findings together, in the case of sympathetic nerve endings, Ca^{2+} elevation coupled to NA release might be derived via Ca^{2+} channels or internal store rather than membrane Na/Ca^{2+} exchange.

Although the type of Ca^{2+} channel for the NA or ACh release differed, involvement of cytosol Ca^{2+} in ouabain-induced neurotransmitter release did not differ between the parasympathetic and sympathetic nerve endings. However, the relation between TTX sensitive Na^+ channel and Ca^{2+} channel opening may differ between the parasympathetic and sympathetic nerve endings. In the present study, ouabain-induced NA efflux was suppressed by ω-conotoxin GVIA but not by TTX, indicating that TTX sensitive depolarization was not involved in Ca^{2+} channel opening coupled to exocytotic NA release. In contrast to NA release,

ouabain-induced ACh release was suppressed by TTX and ω-conotoxin MVIIC, indicating that ouabain-induced depolarization and subsequently ACh release via P/Q type Ca^{2+} channel opening. TTX sensitive or resistant response may be interpreted as two different types of neurotransmitter release mechanisms. Alternatively, ouabain may have induced increases in intraneuronal Na^+ accumulation and elevation of extraneuronal K^+ levels by inhibition of Na^+,K^+-ATPase (D'Ambrosio et al. 2002). Elevations of both intracellular Na^+ and extracellular K^+ exerted regional depolarization following exocytosis via different mechanisms. In the previous study, we demonstrated that high K^+-induced NA release was insensitive to TTX but sensitive to ω-conotoxin GVIA. Furthermore, high K^+ caused a marked increase in dialysate NA but little increase in dialysate Ach (Yamazaki et al. 1998, Kawada et al. 2001). Thus high K^+-induced neurotransmitter release might greatly contribute to the increase in dialysate NA evoked by ouabain but might contribute little to the increase in dialysate ACh.

In conclusion, ouabain alone causes a brisk efflux of NA and ACh from cardiac sympathetic and parasympathetic nerve endings respectively. The ouabain-induced ACh release contributes to the mechanism of ACh exocytosis, which is triggered by centrally mediated or regional depolarization. The regional exocytosis is caused by opening of P/Q type Ca^{2+} channels and/or intracellular Ca^{2+} mobilization from the stored ACh vesicle. The ouabain-induced NA release contributes to the mechanisms of regional exocytosis and/or carrier-mediated outward transport of NA, from stored NA vesicle and/or axoplasma respectively. The regional exocytosis is caused by opening of N type Ca^{2+} channels and intracellular Ca^{2+} mobilization.

Conflict of interest

None.

References

Akiyama, T., Yamazaki, T. & Ninomiya, I. 1991. In vivo monitoring of myocardial interstitial norepinephrine by dialysis technique. Am J Physiol 261, H1643–H1647.

Akiyama, T., Yamazaki, T. & Ninomiya, I. 1994. In vivo detection of endogenous acetylcholine release in cat ventricles. Am J Physiol 266, H854–H860.

Calabresi, P., Marfia, G.A., Centonze, D., Pisani, A. & Bernardi, G. 1999. Sodium influx plays a major role in the membrane depolarization induced by oxygen and glucose deprivation in rat striatal spiny neurons. Stroke 30, 171–190.

Casali, T.A., Gomez, R.S., Moraes-Santos, T. & Gomez, M.V. 1995. Differential effects of calcium channel antagonists on tityustoxin and ouabain-induced release of [3H] acetylcholine from brain cortical slices. Neuropharmacology 34, 599–603.

D'Ambrosio, R., Gordon, D.S. & Winn, H.R. 2002. Differential role of KIR channel and Na(+)/K(+)-pump in the regulation of extracellular K(+) in rat hippocampus. J Neurophysiol 87, 87–102.

Dierkes, P.W., Wusten, H.J., Klees, G., Muller, A. & Hochstrate, P. 2006. Ionic mechanism of ouabian-induced swelling of leech Retzius neurons. Pflugers Arch 452, 25–35.

Edward, C., Dolezal, D., Tucek, S., Zemkova, H. & Vyskocil, F. 1985. Is an acetylcholine transport system responsible for nonquantal release of acetycholine at the rodent myoneural junction? Proc Natl Acad Sci USA 82, 3514–3518.

Gillis, R.A. & Quest, J.A. 1979. The role of the nervous system in the cardiovascular effects of digitalis. Pharmacol Rev 31, 19–97.

Gomez, R.S., Gomez, M.V. & Prado, M.A.M. 1996. Inhibition of Na^+, K^+-ATPase by ouabain opens calcium channels coupled to acetylcholine release in guinea pig myenteric plexus. J Neurochem 66, 1440–1447.

Haass, M., Serf, C., Gerber, S.H. et al. 1997. W. Dual effect of digitalis glycoside on norepinephrine release from human atrial tissue and bovine adrenal chromaffin cells: differential dependence on $[Na+]_i$ and $[Ca2+]_i$. J Mol Cell Cardiol 29, 1615–1627.

Katsuragi, T., Ogawa, S. & Furukawa, T. 1994. Contribution of intra-and extracellular Ca^{2+} to noradrenaline exocytosis induced by ouabain and monesin from guinea-pig vas deferens. Br J Pharmacol 113, 795–800.

Kawada, T., Yamazaki, T., Akiyama, T. et al. 2006. Effects of Ca2+ channel anatagonists on nerve stimulation-induced and ischemia-induced myocardial interstitial acetylcholine release in cats. Am J Physiol 291, H2181–2191.

Kawada, T., Yamazaki, T., Akiyama, T. et al. 2001. In vivo assessment of acetylcholine-releasing function at cardiac vagal nerve terminals. Am J Physiol 281, H139–H145.

Kranzhöfer, R., Haass, M., Kurz, T., Richardt, G. & Schömig, A. 1991. Effect of digitalis glycosides on norepinephrine release in the heart: dual mechanism of action. Circ Res 68, 1628–1637.

McIvor, M.E. & Cummings, C.C. 1987. Sodium fluoride produces a K+ efflux by increasing intracellular Ca2+ through Na+-Ca2+ exchange. Toxicol Lett 38, 169–176.

Nikolsky, E.E., Voronin, V.A. & Vyskocil, F. 1991. Kinetic differences in the effect of calcium on quantal and nonquantal acetylcholine release at the murine diaphragm. Neurosci Lett 123, 192–194.

Nishio, M., Ruch, S.W., Kelly, J.E., Aistrup, G.L., Sheehan, K. & Wasserstrom, J.A. 2004. Ouabain increases sarcoplasmic reticulum calcium release in cardiac myocytes. J Pharmacol Exp Ther 308, 1181–1190.

Satoh, E. & Nakazato, Y. 1992. On the mechanisim of ouabain-induced release of acetylcholine from synaptsomes. J Neurochem 58, 1038–1044.

Sharma, V.K., Pottick, L.A. & Banerjee, S.P. 1980. Ouabain stimulation of noradrenaline transport in guinea pig heart. Nature 286, 817–819.

Ouabain and cardiac autonomic nerve endings · T Yamazaki et al.

Acta Physiol 2007, **191**, 275–284

Smith, D.O. 1992. Routes of actylcholine leakage from cyto-solic and vesicular compartments of rat motor nerve termi-nals. *Neurosci Lett* 135, 5–9.

Sweadner, K. 1985. Ouabain-evoked norepinephrine release from intact rat sympathetic neurons: evidence for carrier-mediated release. *J Neurosci* 5, 2397–2406.

Verbny, Y., Zhang, C.L. & Chiu, S.Y. 2002. Coupling of calcium homeostasis to axonal sodium in axons of mouse optic nerve. *J Neurophysiol* 88, 802–816.

Vizi, E.S. 1998. Differential temperature dependence of carrier-mediated (cytoplasmic) and stimulus-evoked (exocytotic) release of transmitter: a simple method to separate two types of relase. *Neurochem Int* 33, 359–366.

Vyskocil, F. & Illes, P. 1977. Non-quantal release of transmitter at mouse neuromuscular junction and its dependency on the activity of Na$^+$-K$^+$ ATPase. *Pflugers Arch* 370, 295–297.

Wasserstrom, J.A. & Aistrup, G.L. 2005. Digitalis: new actions for an old drug. *Am J Physiol Heart Circ Physiol* 289, H1781–H1793.

Wiedenkeller, D.E. & Sharp, G.W. 1984. Unexpected poten-tiation of insulin release by the calcium store blocker TMB-8. *Endocrinolgy* 114, 116–119.

Yamazaki, T., Akiyama, T., Kitagawa, H., Takauchi, Y., Kawada, T. & Sunagawa, K. 1997. A new, concise dialysis approach to assessment of cardiac sympathetic nerve termi-nal abnormalities. *Am J Physiol* 272, H1182–H1187.

Yamazaki, T., Akiyama, T., Kawada, T. *et al.* 1998. Norepi-nephrine efflux evoked by potassium chloride in cat sym-pathetic nerves: dual mechanism of action. *Brain Res* 794, 146–150.

Yamazaki, T., Akiyama, T. & Mori, H. 2001. Effects of nociceptin on cardiac norepinephrine and acetylcholine release evoked by ouabain. *Brain Res* 904, 153–156.

Zemkova, H., Vyskocil, F. & Edwards, C. 1990. The effect of nerve terminal activity on non-quantal release of acetylcho-line at the mouse neuromuscular junction. *J Physiol* 423, 631–640.

Efferent vagal nerve stimulation induces tissue inhibitor of metalloproteinase-1 in myocardial ischemia-reperfusion injury in rabbit

Kazunori Uemura,[1] Meihua Li,[1] Takaki Tsutsumi,[2] Toji Yamazaki,[3] Toru Kawada,[1] Atsunori Kamiya,[1] Masashi Inagaki,[1] Kenji Sunagawa,[2] and Masaru Sugimachi[1]

Departments of [1]Cardiovascular Dynamics and [3]Cardiac Physiology, National Cardiovascular Center Research Institute, Suita, Japan; and [2]Department of Cardiovascular Medicine, Kyushu University Graduate School of Medical Science, Fukuoka, Japan

Uemura K, Li M, Tsutsumi T, Yamazaki T, Kawada T, Kamiya A, Inagaki M, Sunagawa K, Sugimachi M. Efferent vagal nerve stimulation induces tissue inhibitor of metalloproteinase-1 in myocardial ischemia-reperfusion injury in rabbit. *Am J Physiol Heart Circ Physiol* 293: H2254–H2261, 2007. First published August 10, 2007; doi:10.1152/ajpheart.00490.2007.—Vagal nerve stimulation has been suggested to ameliorate left ventricular (LV) remodeling in heart failure. However, it is not known whether and to what degree vagal nerve stimulation affects matrix metalloproteinase (MMP) and tissue inhibitor of MMP (TIMP) in myocardium, which are known to play crucial roles in LV remodeling. We therefore investigated the effects of electrical stimulation of efferent vagal nerve on myocardial expression and activation of MMPs and TIMPs in a rabbit model of myocardial ischemia-reperfusion (I/R) injury. Anesthetized rabbits were subjected to 60 min of left coronary artery occlusion and 180 min of reperfusion with (I/R-VS, $n = 8$) or without vagal nerve stimulation (I/R, $n = 7$). Rabbits not subjected to coronary occlusion with (VS, $n = 7$) or without vagal stimulation (sham, $n = 7$) were used as controls. Total MMP-9 protein increased significantly after left coronary artery occlusion in I/R-VS and I/R to a similar degree compared with VS and sham values. Endogenous active MMP-9 protein level was significantly lower in I/R-VS compared with I/R. TIMP-1 mRNA expression was significantly increased in I/R-VS compared with the I/R, VS, and sham groups. TIMP-1 protein was significantly increased in I/R-VS and VS compared with the I/R and sham groups. Cardiac microdialysis technique demonstrated that topical perfusion of acetylcholine increased dialysate TIMP-1 protein level, which was suppressed by coperfusion of atropine. Immunohistochemistry demonstrated a strong expression of TIMP-1 protein in cardiomyocytes around the dialysis probe used to perfuse acetylcholine. In conclusion, in a rabbit model of myocardial I/R injury, vagal nerve stimulation induced TIMP-1 expression in cardiomyocytes and reduced active MMP-9.

myocardial remodeling; matrix metalloproteinase; acetylcholine

LEFT VENTRICULAR (LV) myocardial remodeling that occurs after myocardial infarction (MI) leads to progressive LV dilation and eventually pump dysfunction (33, 40). In addition to the loss of contractile cardiomyocytes, pathological degradation and reconstitution of extracellular matrix significantly contribute to the progression of LV remodeling, where matrix metalloproteinase (MMP) and its intrinsic inhibitor, tissue inhibitor of MMP (TIMP), play crucial roles (37, 43).

A previous study using genetically engineered mice demonstrated that target deletion of the MMP-9 gene prevented LV rupture and ameliorated LV remodeling after MI (10). The positive results of MMP inhibition on LV remodeling in animal models led to the proposal to use MMP inhibitors as a potential therapy for patients at risk for the development of heart failure after MI (27, 32). However, recent clinical results from the Prevention of Myocardial Infarction Early Remodeling (PREMIER) trial failed to demonstrate a beneficial effect of MMP inhibition on LV remodeling after MI (16). This indicates the importance of further understanding the in vivo regulatory mechanisms of MMPs to understand and beneficially modify the LV remodeling process.

The cardiac autonomic nervous system plays an important role in the progression of heart failure (21). A previous communication from our laboratory demonstrated that chronic electrical stimulation of vagal nerve ameliorated LV remodeling and markedly improved survival after MI in rat (23). However, it is not known whether and to what degree the vagal nerve affects the MMPs and the TIMPs in vivo. We therefore investigated the effects of electrical stimulation of vagal nerve on myocardial expression of MMP-2/9 and TIMP-1/2 in a rabbit model of myocardial ischemia-reperfusion (I/R) injury. We also investigated the direct action of acetylcholine (ACh), a neurotransmitter released by vagal nerve stimulation (VNS), on myocardial release of TIMP-1 using a cardiac microdialysis technique (19). Our results indicated that VNS induced expression of TIMP-1 from cardiomyocytes and reduced active MMP-9 in myocardial I/R injury in rabbit.

METHODS

We used 49 Japanese white rabbits in this study (male, 2.5–3.0 kg). Care of the animals was in strict accordance with the guiding principles of the Physiological Society of Japan. All protocols were approved by the Animal Subjects Committee of the National Cardiovascular Center.

I/R Study

Experimental preparation. Anesthesia was induced by intravenous injection of pentobarbital sodium (35 mg/kg). Animals were tracheotomized, intubated, and mechanically ventilated. Arterial pH, P_{O_2}, and P_{CO_2} were maintained within the physiological ranges by supplying oxygen and changing the respiratory rate. α-Chloralose (20 $mg \cdot kg^{-1} \cdot h^{-1}$) was continuously infused to maintain an appropriate level of anesthesia during the experiment. A catheter-tipped micromanometer (SPC-330A, Millar Instruments, Houston, TX) was inserted via the right femoral artery to measure arterial pressure (AP). After a median sternotomy, the heart was suspended in a pericardial

---

cradle. Another catheter-tipped micromanometer was introduced into the LV via the apex to measure LV pressure (LVP). Piezoelectric crystals (1 mm, Sonometrics, Ontario, Canada) were attached to the anterior and lateral walls of the LV using cyanoacrylate adhesive (3M, Vetbond, St. Paul, MN) to measure regional LV segmental length. A 4-0 proline suture was passed around the main branch of the left anterior descending coronary artery (LAD), and a snare was formed by passing the ends of the thread through a small vinyl tube. A surface electrocardiogram (ECG) was recorded.

Bilateral cervical vagi were identified and transected at the neck region. A pair of bipolar electrodes was attached at the cardiac end of the right vagal nerve. The duration of electrical pulse used to stimulate the vagal nerve was set at 4 ms. We adjusted the amplitude of the pulse in each animal to reduce heart rate (HR) by 30% from the baseline value at a stimulation frequency of 10 Hz. The resultant stimulation voltage was 2–4 V.

Experimental protocol. Thirty minutes were allowed for stabilization after the initial preparation and surgical procedures were completed. The animals were randomized into the following four groups: *1*) sham group ($n = 7$), in which surgical preparation was conducted without coronary occlusion or vagal stimulation (VS); *2*) VS group ($n = 7$), in which stimulation of the vagal nerve was started after baseline hemodynamics were obtained and continued during the experiment; *3*) I/R group ($n = 7$), in which 60 min of LAD occlusion and 180 min of reperfusion were conducted; and *4*) I/R-VS group ($n = 8$), in which stimulation of the vagal nerve was started 15 min before LAD occlusion and continued throughout 60 min of myocardial ischemia and 180 min of reperfusion.

Baseline hemodynamic data (baseline) were recorded in all groups. A second set of measurements of hemodynamic data (60 min) was obtained during the last 5 min of the 60-min observation period in the sham and VS groups or during the last 5 min of the 60-min ischemic period in the I/R and I/R-VS groups. A third set of measurements of hemodynamic data (240 min) was recorded during the last 5 min of the next 180-min observation period in the sham and VS groups or during the last 5 min of the 180-min reperfusion period in the I/R and I/R-VS groups.

At each time point, hemodynamic data were recorded under a steady-state condition. All data acquisitions were done at end expiration. Analog signals of AP, LVP, segmental length of the anterior-lateral wall of LV (risk area), and ECG were digitized at 200 Hz and stored in a computer for off-line analysis (Sonolab, Sonometrics).

At the end of the experiment, the animal was euthanized. The whole heart was quickly excised and washed with cold PBS. After the vasculature, right ventricular free wall, and atrial appendages were dissected away, the remaining LV wall was snap frozen in liquid nitrogen and stored at $-80°C$.

Myocardial protein extraction. Approximately 200 mg of myocardial tissue sample obtained from the center of the risk area (anterior wall) of the LV free wall was homogenized in 1 ml of lysis buffer containing 50 mmol/l Tris (pH 7.4), 1.5 mmol/l CaCl₂, and 0.5% Triton X-100. The homogenate was centrifuged at 2,000 g for 10 min at 4°C, and the supernatant was collected. Protein concentration of each supernatant sample was determined with a DC Protein assay kit (Bio-Rad, Richmond, CA).

Gelatin zymography. Gelatin zymography was performed to assess the relative contents of the gelatinases MMP-2 and MMP-9 (43). The supernatants (60 μg protein) were loaded in Novex precast 10% Tris-glycine gels containing 0.1% gelatin (Invitrogen, Carlsbad, CA) and then electrophoresed. After renaturation and equilibration, the gels were incubated for 30 h at 37°C in Novex zymogram-developing buffer. The gels were then stained in 0.5% Coomassie blue G-250, dissolved in 30% methanol-10% acetic acid for 60 min, and destained in several changes of methanol-acetic acid for 60 min. Gels were dried and scanned. MMP-2 and MMP-9 related bands were analyzed using the NIH Image software (ImageJ 1.37).

MMP-9 activity assay. Bioactivity assay for MMP-9 was performed using the Biotrak activity assay system (GE Healthcare Bio-Sciences, Piscataway, NJ) following the manufacturer's instructions (42). Briefly, supernatant samples were placed in microtitre well plates coated with anti-MMP-9 (100 μl/well). The plates were incubated overnight at 4°C. The following day, *p*-aminophenylmercuric acetate was added to the wells for measuring "total" MMP-9 (pro- and active MMP-9). Buffer alone was added to the wells for measuring "active" (endogenous active MMP-9) MMP-9. Detection agent was then added to all wells (50 μl/well), and the plate was read at 405 nm ($t = 0$ min) and again after a 2-h incubation at 37°C. The value of MMP-9 was standardized by the protein concentration. All measurements were run in duplicate.

ELISA measurement of TIMP-1 and TIMP-2. Commercially available ELISA kits (Daiichi Fine Chemical, Toyama, Japan) were used to measure TIMP-1 and TIMP-2 levels in supernatants according to the manufacturer's instructions (13, 17, 20). Briefly, standards and samples were incubated in microtitre wells coated with anti-TIMP-1 and anti-TIMP-2 antibody. Peroxidase-labeled antibodies directed to the respective TIMPs were added to the corresponding wells. Visualization of the presence of the peroxidase label was achieved using the *o*-phenylenediamine substrate (TIMP-1) or tetramethylbenzidine substrate (TIMP-2). The plates were read at 490 (TIMP-1) or 450 (TIMP-2) nm. Values of TIMPs were standardized by the protein concentration. Since the ELISA systems have some degree of intraplate and interplate variability (<15%) (7), all measurements were run in duplicate to quadruplicate.

Myocardial RNA extraction and reverse transcription. Total RNA was extracted from the risk area (anterior wall) of the LV free wall by an acid guanidium thiocyanate-phenol chloroform method (Isogen, Nippon Gene). First-strand cDNA was synthesized using reverse transcriptase with random hexamer primers from 1 μg of total RNA in a final volume of 20 μl, according to the manufacturer's protocol (ReverTra Ace, Toyobo).

Real-time quantitative reverse transcription-PCR. To analyze TIMP-1 gene expression in myocardial tissue, real-time polymerase chain reaction (PCR) amplification was performed with SYBR Premix Ex Taq (Perfect Real Time; TaKaRa, Japan) using the ABI PRISM 7500 sequence detection system (Applied Biosystems). For standardization and quantification, rabbit glyceraldehyde 3-phosphate dehydrogenase (GAPDH) was amplified simultaneously. The respective PCR primers were designed from GenBank databases (Table 1). The PCR consisted of initial treatments (50°C, 2 min; and 95°C, 10 min) followed by 40 three-step cycles (denaturation 94°C, 10 s; annealing 60°C, 10 s; and extension 72°C, 40 s). Fluorescence was detected at the end of every extension phase (72°C). After PCR amplification, dissociation curves were constructed to confirm the formation of the intended PCR products. Relative expression of TIMP-1 to the GAPDH levels was calculated as described previously (28, 45).

Hemodynamic data analysis. The following hemodynamic parameters were determined from hemodynamic data: HR, mean arterial pressure, maximum first derivative of LVP (LV dP/dt_{max}), and fractional shortening of anterior-lateral wall (FS). End diastole and end ejection were defined as the peak of R wave of ECG and the peak of minimum first derivative of LVP, respectively. FS was calculated as

Table 1. *Probes used for real-time PCR*

Assay	Sequence	Accession Number
TIMP-1		
Forward	5'-CAACTCCGACCTTGTCATCAG-3'	AY829731
Reverse	5'-GCGTCAAATCCTTTGAACATCT-3'	
GAPDH		
Forward	5'-GGAGAAAGCTGCTAAGTATGACG-3'	L23961
Reverse	5'-CACTGTTGA AGTCGCAGGAG-3'	

TIMP-1, tissue inhibitor of matrix metalloproteinase-1.

the ratio of systolic stroke change in segmental length and end-diastolic length of the anterior-lateral wall (36).

Cardiac Microdialysis Study

Experimental preparation. Experimental preparation was the same as described above in *I/R Study*, except that no coronary artery occlusion was performed. A microdialysis probe was implanted into the LV anterior wall. Heparin sodium (200 U/kg) was administered intravenously to prevent blood coagulation (19).

Dialysis technique. The materials and properties of the dialysis probe have been described (19). Briefly, we designed a hand-made long transverse dialysis probe. One end of a polyethylene tube (25 cm long, 0.5 mm OD, and 0.2 mm ID) was dilated with a 27-gauge needle (0.4 mm OD). Each end of the dialysis fiber (8 mm long, 0.215 mm OD, 0.175 mm ID, and 300 Å pore size; Evaflux type 5A, Kuraray Medical, Tokyo, Japan) was inserted into the polyethylene tube and glued.

Recovery of TIMP-1 passing through the dialysis fiber membrane was evaluated in vitro. The dialysis probe ($n = 4$) was immersed in Ringer solution (in mM; 147.0 NaCl, 4.0 KCl, and 2.25 $CaCl_2$) containing Tween 20 (0.1%) and various concentrations of TIMP-1 (10–40 ng/ml, free form of human TIMP-1, Daiichi Fine Chemical). The dialysis probe was perfused with Ringer solution at a rate of 2.5 μl/min using a microinjection pump (model CMA/102, Carnegie Medicine). We measured the concentration of TIMP-1 in the dialysate sample using an ELISA kit. The relative recovery of TIMP-1 was calculated as the ratio of TIMP-1 concentration in dialysate to its concentration in the medium surrounding the probe (11, 22). The relative recovery of TIMP-1 was $11.1 \pm 0.3\%$. Recovery was constant between probes and within the probe for the TIMP-1 concentration range studied.

A fine-guiding needle (25 mm long, 0.51 mm OD, and 0.25 mm ID) was used for implantation of the dialysis probes. The guiding needle was connected to the dialysis probe with a stainless steel rod (5 mm long and 0.25 mm OD). Experimental protocols were initiated 2 h after implanting the dialysis probe. The dialysate sampling period was set at 60 min and was performed taking into account the dead space volume between the dialysis membrane and the sample tube.

Experimental protocol. After baseline dialysate was sampled and baseline hemodynamic data were recorded, the animals were randomized into the following three groups: *1*) VNS group ($n = 5$), in which electrical stimulation of vagal nerve was performed while the LV wall was perfused with Ringer solution via the dialysis probe; *2*) ACh group ($n = 8$), in which the LV wall was perfused with Ringer solution containing ACh (1 mM); and *3*) ACh-atropine (Atr) group ($n = 7$), in which the LV wall was perfused with Ringer solution containing ACh (1 mM) and Atr (0.2 mM). At 150 min after randomization, dialysate sampling and hemodynamic data recording were performed.

At the end of the experiment, the animal was euthanized. From selected hearts, transmural blocks of the LV free wall containing the dialysis probe were fixed in 4% paraformaldehyde for immunohistochemistry.

Immunohistochemistry and confocal microscopy. To investigate the distribution of TIMP-1, we performed confocal image analysis of LV tissue stained with anti-TIMP-1 antibody. Fixed blocks of LV tissues were washed in 0.1 mol/l phosphate buffer (pH 7.4), embedded in paraffin, and sectioned at a thickness of 5 μm. Sections were deparaffinized using xylene, rehydrated with serial grades of ethanol, and followed by hydration with distilled water. For antigen retrieval of TIMP-1 protein, specimens were immersed in a vessel filled with Target Retrieval Solution (pH 6.1; DAKO). The vessel containing the specimens was autoclaved at 121°C for 20 min. The slides were then allowed to cool at room temperature for 20 min to complete antigen unmasking. The sections were then incubated for 30 h with a mouse anti-TIMP-1 antibody (7-6C1, Daiichi Fine Chemical) diluted 1:5 and

then incubated for 2 h in Alexa-488-conjugated goat anti-mouse Ig-G (Molecular Probes) diluted 1:200. Fluorescence of Alexa-488 was observed with a confocal laser-scanning microscope system (FV 300, Olympus). Reconstructed projection images were obtained from serial optical sections recorded at an interval of 0.5 μm.

Exclusion Criteria

Animals were excluded from the study when the following criteria were met: *1*) in the I/R study, coronary artery occlusion did not produce substantial regional dysfunction (FS of the risk area after occlusion was not <20% of the baseline value); *2*) intractable ventricular fibrillation or atrial tachycardia occurred; and *3*) the animal died during the surgical procedure, and the protocol was not completed.

Statistical Analysis

All data are presented as means $\pm$ SE. Tukey-Welsch's step-down multiple comparison test was used to determine the significance of differences among groups. P values <0.05 were considered statistically significant.

RESULTS

I/R Study

As shown in Fig. 1A, zymography of the myocardial extracts detected two bands at 92 and 72 kDa, corresponding to MMP-9 and MMP-2, respectively. Densitometric analysis demonstrated that relative MMP-9 level increased to a similar degree in the I/R and I/R-VS groups compared with the sham and VS groups (Fig. 1B). The relative MMP-2 level decreased in the I/R group compared with the sham and I/R-VS groups (Fig. 1C).

Bioactivity assays demonstrated that myocardial levels of total MMP-9 protein increased to a similar degree in the I/R and I/R-VS groups compared with sham and VS groups (Fig. 2A). Levels of endogenous active MMP-9 protein also increased in the I/R and I/R-VS groups compared with the sham and VS groups (Fig. 2B). The level of active MMP-9 in the I/R-VS group was significantly lower than that in the I/R group ($<50\%$, $P < 0.01$).

The myocardial level of TIMP-1 protein increased in the VS and I/R-VS groups compared with the sham and I/R groups (Fig. 3A). There was no significant difference in the myocardial level of TIMP-2 protein among the four groups (Fig. 3B). TIMP-1 mRNA as measured by real-time RT-PCR was increased in the I/R-VS group compared with the sham, VS, and I/R groups (Fig. 3C).

Table 2 summarizes the data of systemic hemodynamics and LV function during the I/R study. In the VS and I/R-VS groups, HR decreased significantly compared with sham and I/R values at 60 and 240 min. In the I/R and I/R-VS groups, FS was depressed during ischemia with only partial recovery after reperfusion. In the I/R and I/R-VS groups, sonomicrometry demonstrated early systolic bulging of the anterior LV wall during ischemia as reflected by negative FS at the 60-min time point. There was no significant difference in LV dP/dt_{max} and FS between the I/R and I/R-VS groups at 60 and 240 min.

Cardiac Microdialysis Study

Figure 4 presents dialysate TIMP-1 concentrations in response to electrical stimulation of the vagal nerve, to perfusion of ACh, and to perfusion of ACh with Atr. There were no
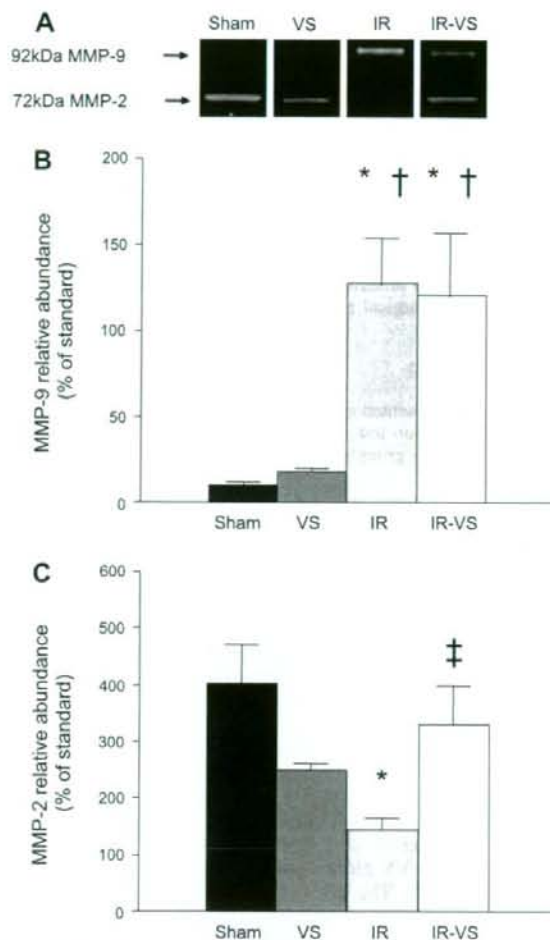
Fig. 1. Zymographic analysis of matrix metalloproteinase (MMP)-9 and -2 proteins in isolated myocardium. Sham, no myocardial ischemia and no vagal stimulation; VS, no myocardial ischemia with vagal stimulation; I/R, myocardial ischemia-reperfusion; I/R-VS, myocardial ischemia-reperfusion with VS. A: representative zymogram showing MMP-9 at 92 kDa and MMP-2 at 72 kDa. B: densitometric analysis of relative MMP-9 content expressed as percentage of standard. C: densitometric analysis of relative MMP-2 content expressed as percentage of standard. Data are means ± SE. *$P < 0.01$ vs. sham; †$P < 0.01$ vs. VS; ‡$P < 0.05$ vs. I/R.

significant differences in baseline TIMP-1 concentrations among the three groups. At 150 min, dialysate TIMP-1 concentration was significantly higher in the VNS and ACh groups than in the ACh-Atr group ($P < 0.05$).

Figure 5 depicts representative microscopic findings of LV tissue around the microdialysis probes in the VNS, ACh, and ACh-Atr groups. Hematoxylin-eosin-stained sections demonstrated only a minimum hemorrhage around the dialysis probe (Fig. 5, A–C). TIMP-1-positive cardiomyocytes were detected sparsely but in diffuse distribution throughout the myocardium in the VNS group (Fig. 5D). TIMP-1-positive cardiomyocytes were detected over a relatively wide area around the dialysis probe in the ACh group (Fig. 5E). TIMP-1-positive cardiomyocytes were also detected but localized close to the dialysis

probe in the ACh-Atr group (Fig. 5F). Immunoreactive signals of TIMP-1 were restricted to the cytoplasm of cardiomyocytes in all the groups (Fig. 5, G–I).

Table 3 summarizes the data of systemic hemodynamics and LV function during the cardiac microdialysis study. In the VNS group, HR decreased significantly compared with that in the ACh and ACh-Atr groups at 150 min. In the ACh and ACh-Atr groups, topical perfusion of ACh or ACh with Atr did not affect the systemic hemodynamics and the LV functions. Except for HR, there were no significant differences in other hemodynamic parameters among the three groups.

DISCUSSION

The major new findings of the present study were as follows. In ischemia-reperfused myocardium, stimulation of the efferent vagal nerve increased TIMP-1 mRNA and protein levels and reduced endogenous active MMP-9 protein. In normal myocardium, VNS or topical perfusion of ACh through a microdialysis probe increased dialysate TIMP-1 protein level. An increase in the dialysate TIMP-1 protein level induced by ACh perfusion was suppressed by coperfusion of Atr.

The robust increase in total MMP-9 levels after reperfusion in this study (Figs. 1B and 2A) might be mainly due to the
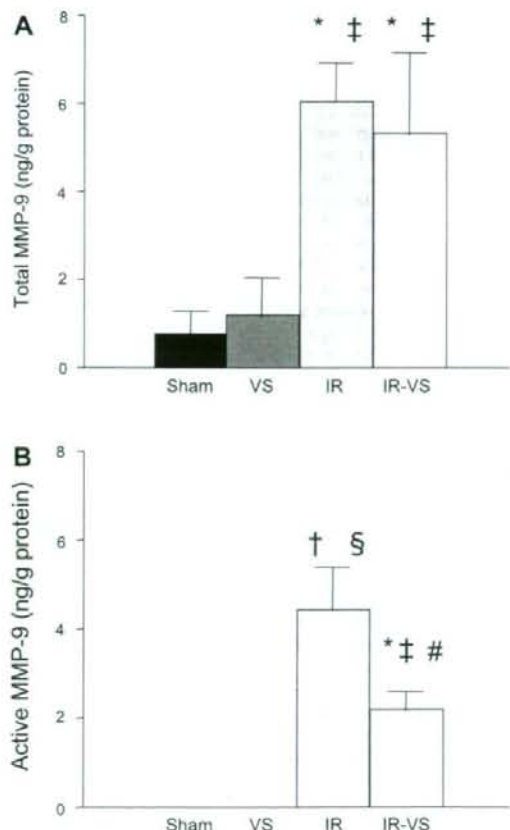

Fig. 2. Bioactivity assay of total (A) and active (B) MMP-9 protein. *$P < 0.05$; †$P < 0.01$ vs. sham; ‡$P < 0.05$; §$P < 0.01$ vs. VS. #$P < 0.01$ vs. I/R.
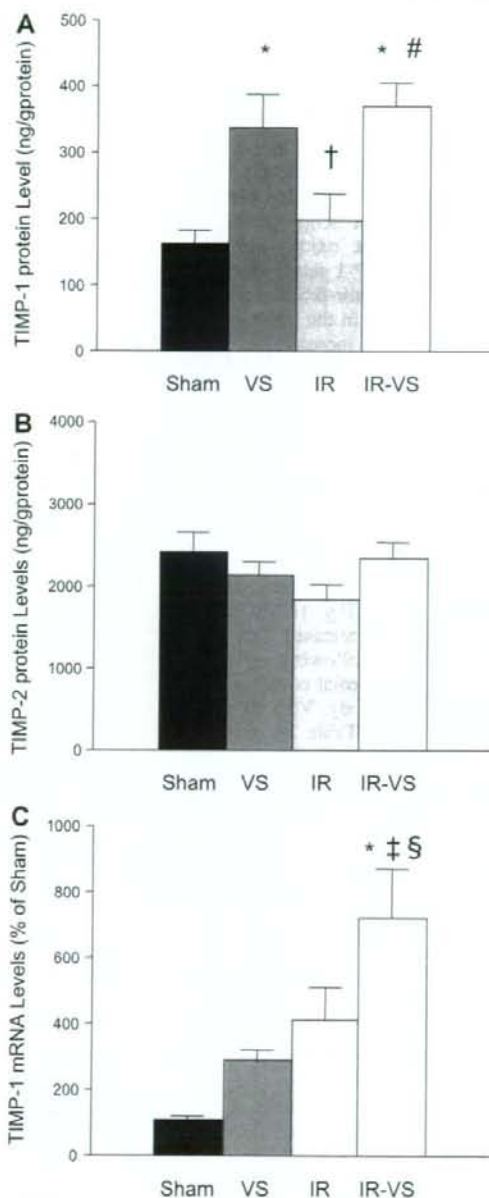
A

B

C

Fig. 3. ELISA measurement of tissue inhibitor of MMP (TIMP)-1 (*A*) and -2 (*B*) protein. Real-time RT-PCR analysis of TIMP-1 mRNA expressed as percentage of sham (*C*). *$P < 0.01$ vs. sham; †$P < 0.05$; ‡$P < 0.01$ vs. VS; §$P < 0.05$; #$P < 0.01$ vs. I/R.

Table 2. *Hemodynamic parameters during I/R study*

	Baseline	60 min	240 min
HR, beats/min			
Sham	317±9	334±7	326±9
VS	281±14	215±17*‡	238±19*‡
I/R	306±9	316±9	314±8
I/R-VS	301±7	217±5*‡	228±8*‡
MAP, mmHg			
Sham	92±3	93±4	92±3
VS	98±4	91±5	89±5
I/R	102±3	95±4	88±6
I/R-VS	99±4	88±4	83±2
LV dP/dt_{max}, mmHg/s			
Sham	5,119±263	5,308±388	4,819±339
VS	5,040±381	3,993±319	4,140±302
I/R	5,524±423	5,276±404	4,514±467
I/R-VS	5,672±360	4,549±250	4,079±188
FS, %			
Sham	10.8±0.9	10.1±1.0	9.3±1.0
VS	12.2±1.1	11.1±1.2	10.4±1.6
I/R	8.7±0.8	−0.6±0.6*†	0.1±0.8*†
I/R-VS	8.5±1.3	−0.6±0.4*†	1.5±0.7*†

Values are means ± SE. Sham group, no myocardial ischemia and no vagal stimulation (VS); VS group, no myocardial ischemia with VS; I/R group, myocardial ischemia-reperfusion (I/R); I/R-VS, myocardial I/R with VS; HR, heart rate; MAP, mean arterial pressure; LV dP/dt_{max}, maximum first derivative of left ventricular (LV) pressure; FS, fractional shortening of anterior wall (risk area). *$P < 0.01$ vs. sham; †$P < 0.01$ vs. VS; ‡$P < 0.01$ vs. I/R.

active MMP-9 itself more potently than in the case without VNS (14). Oxygen free radical induces expression and activation of MMP-9 (17, 41). Reduction of HR by VNS probably reduced myocardial oxygen consumption, ameliorated myocardial ischemia, and reduced oxygen free radicals (30). This may contribute to some extent to the reduction of active MMP-9 in the I/R-VS group.

In the I/R study, TIMP-1 mRNA was significantly higher in the I/R-VS group compared with the sham, VS, and I/R groups (Fig. 3C). TIMP-1 mRNA appeared higher in the VS and I/R groups compared with the sham group, although the differences were not significant. Stapel et al. (38) noted increased expression of TIMP-1 mRNA after myocardial I/R in mice. Proinflammatory cytokines such as interleukin-1β induced by
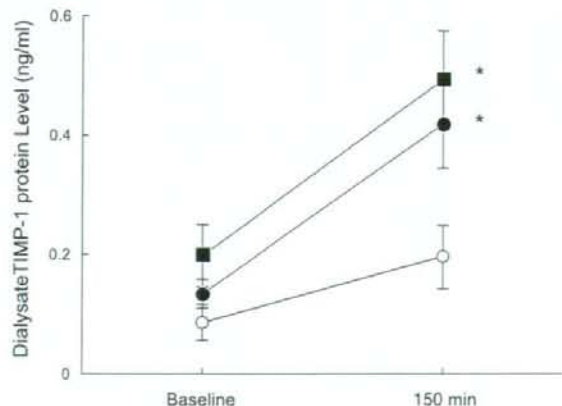

Fig. 4. Dialysate TIMP-1 protein concentration in response to vagal nerve stimulation (■), perfusion of acetylcholine (ACh; ●), or ACh with atropine (Atr) (○). *$P < 0.05$ vs. perfusion of ACh with Atr.

infiltrated neutrophils. Although all cell types, including cardiomyocytes (25, 34) and endothelial cells (41), express MMP-9, neutrophil is an important source of MMP-9 after I/R (26). The level of endogenous active MMP-9 was lower in the I/R-VS group than in the I/R group (Fig. 2B). Increased expression of TIMP-1 by VNS (Fig. 3) likely inhibited the conversion of pro-MMP-9 to active MMP-9 and/or inhibited
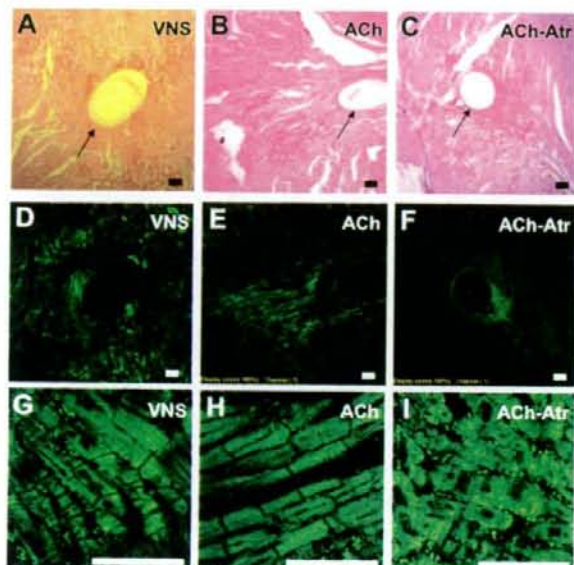
Fig. 5. Representative microscopic finding of left ventricular (LV) tissue implanted with microdialysis probe. *A–C*: hematoxylin and eosin-stained section of LV tissue perfused with Ringer solution under vagal nerve stimulation (VNS; *A*), perfused with ACh (*B*), and perfused with ACh and Atr (ACh-Atr; *C*). *D–F*: anti-TIMP-1 antibody (green)-immunostained sections of LV tissue perfused with Ringer solution under VNS (*D*), perfused with ACh (*E*), and perfused with ACh-Atr (*F*). *G–I*: higher magnifications of *D–F*, respectively. Arrows indicate dialysis probes. Bar = 100 μm.

myocardial ischemia are known to induce TIMP-1 (4). VNS and myocardial ischemia likely exerted an additive effect on the induction of TIMP-1 mRNA in the I/R-VS group. TIMP-1 protein levels in the VS and I/R-VS groups were significantly elevated compared with the sham and I/R groups (Fig. 3*A*). Figure 3, *A* and *C*, indicates dissociation between TIMP-1 mRNA and protein synthesis among the four groups. If the TIMP-1 protein level had correlated with the mRNA level, TIMP-1 protein level in the I/R and I/R-VS groups should have been higher than those presented in Fig. 3*A*. In myocardial ischemia, protein synthesis decreases owing to the inhibition of peptide chain elongation (8, 18). This may have partially inhibited TIMP-1 protein synthesis in the I/R and I/R-VS groups.

In the cardiac microdialysis study, the ACh-induced release of TIMP-1 was mediated by muscarinic ACh receptors because Atr blocked the increase in TIMP-1 in response to ACh stimulation (Fig. 4). TIMP-1 was produced by cardiomyocytes (Fig. 5, *G–I*). These findings suggest that VNS may induce TIMP-1 mRNA expression through muscarinic ACh receptors in cardiomyocytes and increase TIMP-1 protein content in myocardium. The distribution of TIMP-1-positive cardiomyocytes was different among the three groups (Fig. 5, *D–F*). This may reflect differences in the distribution of ACh among the three groups. ACh probably had a diffuse distribution in the myocardium in the VNS group but was concentrated around the dialysis probe in ACh group, whereas the effect of ACh concentrated around the dialysis probe was antagonized by Atr in the ACh-Atr group.

In addition to cardiomyocytes (25, 34), a variety of cell types, such as fibroblasts (14) and endothelial cells (6), produces and secretes TIMP-1. TIMP-1 expression in these cell types is low in the basal condition but is transcriptionally induced by various agents, including the cytokines, serum, growth factors, and phorbol esters (14). The signal transduction pathway from muscarinic ACh receptor stimulation to the induction of the TIMP-1 gene is not clear. Further elucidation of this is not in the scope of this study. ACh increases the production of nitric oxide from cardiomyocytes (9). Nitric oxide induces TIMP-1 gene expression by activating the transforming growth factor-β/Smad signaling pathway in glomerular mesangial cells in the kidney (2). These mechanisms may be involved in the increases in TIMP-1 mRNA and protein induced by VNS in myocardial I/R observed in the present study. Further studies are clearly required to elucidate these issues.

Myocardial expression of TIMP-2 was not modified by VNS (Fig. 3*B*). Contrary to the highly responsive nature of TIMP-1 expression to stimuli, TIMP-2 expression is, for the most part, constitutive (14). Previous studies demonstrated that ischemic injury or change in loading condition had little effect on myocardial expression of TIMP-2 (24, 25, 29). Myocardial content of MMP-2 decreased after I/R, and the decrease was inhibited by VNS (Fig. 1*C*). Cheung et al. (5) demonstrated that MMP-2 was released from the myocardium into the coronary effluent following myocardial I/R, resulting in the depletion of myocardial content of MMP-2.

In the present study, VNS did not prevent contractile dysfunction after I/R (Table 2). Actions of MMP and TIMP did not seem to be responsible for acute mechanical changes. Lu et al. (29) demonstrated that treatment with the MMP inhibitor failed to prevent acute myocardial dysfunction and regional expansion after I/R injury. The duration of reperfusion in our study (180 min) and that in Lu et al. (90 min) (29) may be too short to detect a significant influence of MMP and TIMP on regional LV function, which may become evident after a longer period of reperfusion.

Table 3. *Hemodynamic parameters during cardiac microdialysis study*

	Baseline	150 min
HR, beat/min		
VNS	286 ± 7	$227 \pm 7 *†$
ACh	303 ± 16	308 ± 9
ACh-Atr	304 ± 14	298 ± 16
MAP, mmHg		
VNS	101 ± 8	103 ± 8
ACh	93 ± 3	100 ± 4
ACh-Atr	87 ± 3	92 ± 6
LV dP/dt_{max}, mmHg/s		
VNS	$5,050 \pm 588$	$4,768 \pm 475$
ACh	$5,203 \pm 345$	$5,488 \pm 400$
ACh-Atr	$4,519 \pm 269$	$4,718 \pm 450$
FS, %		
VNS	7.4 ± 1.8	7.2 ± 1.9
ACh	5.0 ± 1.2	4.9 ± 1.2
ACh-Atr	5.4 ± 0.5	5.0 ± 0.5

Values are means $\pm$ SE. VNS group, LV tissue was perfused with Ringer solution via a dialysis probe under vagal nerve stimulation; ACh group, LV tissue was perfused with Ringer solution containing ACh (1 mM) via a dialysis probe; ACh-Atr group, LV tissue was perfused with ACh (1 mM) and atropine (0.2 mM) via a dialysis probe. *$P < 0.01$ vs. ACh; †$P < 0.01$ vs. ACh-Atr.

Several previous studies (10, 35, 39) demonstrated that targeted deletion of MMP-9 and/or the upregulation of TIMP-1 reduced infarct size, prevented LV rupture, and ameliorated LV remodeling after MI. Conversely, the expression of other MMPs, such as MMP-2, has been shown to be important in the myocardial healing that occurs in the later phases after ischemic injury (10). These observations suggest that the beneficial effect of VNS on LV remodeling after MI observed in our previous study (23) may be in a part mediated through the modified expression of MMPs and TIMPs as noted in the present study.

Except for the post-MI LV remodeling, MMPs and TIMPs contribute to the progression of various cardiovascular disorders, including expansion and rupture of aortic aneurysm (44), progression of acute viral myocarditis (15), and restenosis after coronary intervention (12). Local overexpression of TIMP-1 prevented the expansion and rupture of aortic aneurysm in rats (3) or prevented cardiac injury and dysfunction during experimental viral myocarditis in mice (15). VNS may be an effective biological inducer of TIMP-1 for the treatment of these disorders.

Limitation

The present study examined a limited number of MMP and TIMP species over a very short duration after myocardial I/R. A number of MMP and TIMP species are expressed in the myocardium, and several have been identified to be upregulated in cardiac disorders (24). Myocardial MMP-1 (collagenase) is induced by I/R (29). The actions of MMP-1 are inhibited in part by TIMP-1 (31). These suggest that VNS may inhibit the activity of MMP-1 in myocardial I/R injury. Further studies to define the effect of VNS on the profile of MMPs and TIMPs expressed in the myocardium are warranted.

In the present study, VNS was started 15 min before coronary occlusion. We did not examine whether VNS started after the coronary artery occlusion or whether reperfusion is capable of increasing myocardial TIMP-1. The pretreatment strategy as adopted in this study is unrealistic in clinical practice. Therefore, further studies are required to examine the time factor of VNS.

Concentration of ACh perfused through the dialysis probe in this study (1 mM) was substantially higher than the dialysate concentration of endogenous ACh released from the myocardium (<20 nM) (1). The ACh concentration within the myocardial interstitium might have been elevated over the supraphysiological range in the present microdialysis study. However, even if the interstitial concentration of ACh was unphysiologically high, Atr blocked the increase in TIMP-1 expression in response to ACh stimulation. Therefore, it is fair to say that TIMP-1 expression in response to ACh stimulation is mediated through the muscarinic ACh receptor.

TIMP-1 binds with MMPs to form a rather high molecular weight complex. Our preliminary in vitro experiment demonstrated that the relative recovery of TIMP-1/lipocalin/MMP-9 complex (Calbiochem, La Jolla, CA) was $3.8 \pm 1.3\%$ (range 0–5.5%) and was lower than that for free TIMP-1 ($11.1 \pm 0.3\%$) (see METHODS). Although the presence of MMPs, especially MMP-9, could affect the measurement of TIMP-1 within the myocardium by our microdialysis method, this probably does not affect the conclusion drawn from the cardiac micro-

dialysis study, because the study was conducted in a heart free of I/R, which might contain low levels of myocardial MMP-9 as inferred from the results of the I/R study.

CONCLUSION

In a rabbit model of myocardial I/R injury, VNS induced TIMP-1 expression in cardiomyocytes and reduced active MMP-9.

GRANTS

REFERENCES

1. **Akiyama T, Yamazaki T.** Adrenergic inhibition of endogenous acetylcholine release on postganglionic cardiac vagal nerve terminals. *Cardiovasc Res* 46: 531–538, 2000.
2. **Akool el-S, Doller A, Muller R, Gutwein P, Xin C, Huwiler A, Pfeilschifter J, Eberhardt W.** Nitric oxide induces TIMP-1 expression by activating the transforming growth factor beta-Smad signaling pathway. *J Biol Chem* 280: 39403–39416, 2005.
3. **Allaire E, Forough R, Clowes M, Starcher B, Clowes AW.** Local overexpression of TIMP-1 prevents aortic aneurysm degeneration and rupture in a rat model. *J Clin Invest* 102: 1413–1420, 1998.
4. **Chandrasekar B, Smith JB, Freeman GL.** Ischemia-reperfusion of rat myocardium activates nuclear factor-KappaB and induces neutrophil infiltration via lipopolysaccharide-induced CXC chemokine. *Circulation* 103: 2296–2302, 2001.
5. **Cheung PY, Sawicki G, Wozniak M, Wang W, Radomski MW, Schulz R.** Matrix metalloproteinase-2 contributes to ischemia-reperfusion injury in the heart. *Circulation* 101: 1833–1839, 2000.
6. **Chua CC, Hamdy RC, Chua BH.** Angiotensin II induces TIMP-1 production in rat heart endothelial cells. *Biochim Biophys Acta* 1311: 175–180, 1996.
7. **Chua PK, Melish ME, Yu Q, Yanagihara R, Yamamoto KS, Nerurkar VR.** Elevated levels of matrix metalloproteinase 9 and tissue inhibitor of metalloproteinase 1 during the acute phase of Kawasaki disease. *Clin Diagn Lab Immunol* 10: 308–314, 2003.
8. **Crozier SJ, Vary TC, Kimball SR, Jefferson LS.** Cellular energy status modulates translational control mechanisms in ischemic-reperfused rat hearts. *Am J Physiol Heart Circ Physiol* 289: H1242–H1250, 2005.
9. **Dedkova EN, Ji X, Wang YG, Blatter LA, Lipsius SL.** Signaling mechanisms that mediate nitric oxide production induced by acetylcholine exposure and withdrawal in cat atrial myocytes. *Circ Res* 93: 1233–1240, 2003.
10. **Ducharme A, Frantz S, Aikawa M, Rabkin E, Lindsey M, Rohde LE, Schoen FJ, Kelly RA, Werb Z, Libby P, Lee RT.** Targeted deletion of matrix metalloproteinase-9 attenuates left ventricular enlargement and collagen accumulation after experimental myocardial infarction. *J Clin Invest* 106: 55–62, 2000.
11. **Ergul A, Walker CA, Goldberg A, Baicu SC, Hendrick JW, King MK, Spinale FG.** ET-1 in the myocardial interstitium: relation to myocyte ECE activity and expression. *Am J Physiol Heart Circ Physiol* 278: H2050–H2056, 2000.
12. **Feldman LJ, Mazighi M, Scheuble A, Deux JF, De Benedetti E, Badier-Commander C, Brambilla E, Henin D, Steg PG, Jacob MP.** Differential expression of matrix metalloproteinases after stent implantation and balloon angioplasty in the hypercholesterolemic rabbit. *Circulation* 103: 3117–3122, 2001.
13. **Fujimoto N, Zhang J, Iwata K, Shinya T, Okada Y, Hayakawa T.** A one-step sandwich enzyme immunoassay for tissue inhibitor of metalloproteinases-2 using monoclonal antibodies. *Clin Chim Acta* 220: 31–45, 1993.
14. **Gomez DE, Alonso DF, Yoshiji H, Thorgeirsson UP.** Tissue inhibitors of metalloproteinases: structure, regulation and biological functions. *Eur J Cell Biol* 74: 111–122, 1997.

15. Heymans S, Pauschinger M, De Palma A, Kallwellis-Opara A, Rutschow S, Swinnen M, Vanhoutte D, Gao F, Torpai R, Baker AH, Padalko E, Neyts J, Schultheiss HP, Van de Werf F, Carmeliet P, Pinto YM. Inhibition of urokinase-type plasminogen activator or matrix metalloproteinases prevents cardiac injury and dysfunction during viral myocarditis. Circulation 114: 565–573, 2006.

16. Hudson MP, Armstrong PW, Ruzyllo W, Brum J, Cusmano L, Krzeski P, Lyon R, Quinones M, Theroux P, Sydlowski D, Kim HE, Garcia MJ, Jaber WA, Weaver WD. Effects of selective matrix metalloproteinase inhibitor (PG-116800) to prevent ventricular remodeling after myocardial infarction: results of the PREMIER (Prevention of Myocardial Infarction Early Remodeling) trial. J Am Coll Cardiol 48: 15–20, 2006.

17. Kameda K, Matsunaga T, Abe N, Hanada H, Ishizaka H, Ono H, Saitoh M, Fukui K, Fukuda I, Osanai T, Okumura K. Correlation of oxidative stress with activity of matrix metalloproteinase in patients with coronary artery disease. Possible role for left ventricular remodelling. Eur Heart J 24: 2180–2185, 2003.

18. Kao R, Rannels DE, Morgan HE. Effects of anoxia and ischemia on protein synthesis in perfused rat hearts. Circ Res 38, Suppl 1: I124–I130, 1976.

19. Kitagawa H, Yamazaki T, Akiyama T, Sugimachi M, Sunagawa K, Mori H. Microdialysis separately monitors myocardial interstitial myoglobin during ischemia and reperfusion. Am J Physiol Heart Circ Physiol 289: H924–H930, 2005.

20. Kodama S, Iwata K, Iwata H, Yamashita K, Hayakawa T. Rapid one-step sandwich enzyme immunoassay for tissue inhibitor of metalloproteinases. An application for rheumatoid arthritis serum and plasma. J Immunol Methods 127: 103–108, 1990.

21. La Rovere MT, Bigger JT Jr, Marcus FI, Mortara A, Schwartz PJ. Baroreflex sensitivity and heart-rate variability in prediction of total cardiac mortality after myocardial infarction. ATRAMI (Autonomic Tone and Reflexes After Myocardial Infarction) Investigators. Lancet 351: 478–484, 1998.

22. Le Quellec A, Dupin S, Genissel P, Saivin S, Marchand B, Houin G. Microdialysis probes calibration: gradient and tissue dependent changes in no net flux and reverse dialysis methods. J Pharmacol Toxicol Methods 33: 11–16, 1995.

23. Li M, Zheng C, Sato T, Kawada T, Sugimachi M, Sunagawa K. Vagal nerve stimulation markedly improves long-term survival after chronic heart failure in rats. Circulation 109: 120–124, 2004.

24. Li YY, Feldman AM, Sun Y, McTiernan CF. Differential expression of tissue inhibitors of metalloproteinases in the failing human heart. Circulation 98: 1728–1734, 1998.

25. Li YY, Feng Y, McTiernan CF, Pei W, Moravec CS, Wang P, Rosenblum W, Kormos RL, Feldman AM. Downregulation of matrix metalloproteinases and reduction in collagen damage in the failing human heart after support with left ventricular assist devices. Circulation 104: 1147–1152, 2001.

26. Lindsey M, Wedin K, Brown MD, Keller C, Evans AJ, Smolen J, Burns AR, Rossen RD, Michael L, Entman M. Matrix-dependent mechanism of neutrophil-mediated release and activation of matrix metalloproteinase 9 in myocardial ischemia/reperfusion. Circulation 103: 2181–2187, 2001.

27. Lindsey ML, Gannon J, Aikawa M, Schoen FJ, Rabkin E, Lopresti-Morrow L, Crawford J, Black S, Libby P, Mitchell PG, Lee RT. Selective matrix metalloproteinase inhibition reduces left ventricular remodeling but does not inhibit angiogenesis after myocardial infarction. Circulation 105: 753–758, 2002.

28. Livak KJ, Schmittgen TD. Analysis of relative expression data using real-time quantitative PCR and the $2^{-\Delta\Delta C_T}$ method. Methods 25: 402–408, 2001.

29. Lu L, Gunja-Smith Z, Woessner JF, Ursell PC, Nissen T, Galardy RE, Xu Y, Zhu P, Schwartz GG. Matrix metalloproteinases and collagen ultrastructure in moderate myocardial ischemia and reperfusion in vivo. Am J Physiol Heart Circ Physiol 279: H601–H609, 2000.

30. Mioni C, Bazzani C, Giuliani D, Altavilla D, Leone S, Ferrari A, Minutoli L, Bitto A, Marini H, Zaffe D, Botticelli AR, Iannone A, Tomasi A, Bigiani A, Bertolini A, Squadrito F, Guarini S. Activation of an efferent cholinergic pathway produces strong protection against myocardial ischemia/reperfusion injury in rats. Crit Care Med 33: 2621–2628, 2005.

31. Moe SM, Singh GK, Bailey AM. Beta2-microglobulin induces MMP-1 but not TIMP-1 expression in human synovial fibroblasts. Kidney Int 57: 2023–2034, 2000.

32. Mukherjee R, Brinsa TA, Dowdy KB, Scott AA, Baskin JM, Deschamps AM, Lowry AS, Escobar GP, Lucas DG, Yarbrough WM, Zile MR, Spinale FG. Myocardial infarct expansion and matrix metalloproteinase inhibition. Circulation 107: 618–625, 2003.

33. Pfeffer MA, Braunwald E. Ventricular remodeling after myocardial infarction. Experimental observations and clinical implications. Circulation 81: 1161–1172, 1990.

34. Romanic AM, Burns-Kurtis CL, Gout B, Berrebi-Bertrand I, Ohlstein EH. Matrix metalloproteinase expression in cardiac myocytes following myocardial infarction in the rabbit. Life Sci 68: 799–814, 2001.

35. Romanic AM, Harrison SM, Bao W, Burns-Kurtis CL, Pickering S, Gu J, Grau E, Mao J, Sathe GM, Ohlstein EH, Yue TL. Myocardial protection from ischemia/reperfusion injury by targeted deletion of matrix metalloproteinase-9. Cardiovasc Res 54: 549–558, 2002.

36. Silvestry SC, Taylor DA, Lilly RE, Atkins BZ, Marathe US, Davis JW, Kraus W, Glower DD. The in vivo quantification of myocardial performance in rabbits: a model for evaluation of cardiac gene therapy. J Mol Cell Cardiol 28: 815–823, 1996.

37. Squire IB, Evans J, Ng LL, Loftus IM, Thompson MM. Plasma MMP-9 and MMP-2 following acute myocardial infarction in man: correlation with echocardiographic and neurohumoral parameters of left ventricular dysfunction. J Card Fail 10: 328–333, 2004.

38. Stapel H, Kim SC, Osterkamp S, Knuefermann P, Hoeft A, Meyer R, Grohe C, Baumgarten G. Toll-like receptor 4 modulates myocardial ischaemia-reperfusion injury: role of matrix metalloproteinases. Eur J Heart Fail 8: 665–672, 2006.

39. Trescher K, Bernecker O, Fellner B, Gyongyosi M, Schafer R, Aharinejad S, DeMartin R, Wolner E, Podesser BK. Inflammation and postinfarct remodeling: overexpression of IkappaB prevents ventricular dilation via increasing TIMP levels. Cardiovasc Res 69: 746–754, 2006.

40. Udelson JE, Konstam MA. Relation between left ventricular remodeling and clinical outcomes in heart failure patients with left ventricular systolic dysfunction. J Card Fail 8: S465–S471, 2002.

41. Uemura S, Matsushita H, Li W, Glassford AJ, Asagami T, Lee KH, Harrison DG, Tsao PS. Diabetes mellitus enhances vascular matrix metalloproteinase activity: role of oxidative stress. Circ Res 88: 1291–1298, 2001.

42. Verheijen JH, Nieuwenbroek NM, Beekman B, Hanemaaijer R, Verspaget HW, Ronday HK, Bakker AH. Modified proenzymes as artificial substrates for proteolytic enzymes: colorimetric assay of bacterial collagenase and matrix metalloproteinase activity using modified prourokinase. Biochem J 323: 603–609, 1997.

43. Webb CS, Bonnema DD, Ahmed SH, Leonardi AH, McClure CD, Clark LL, Stroud RE, Corn WC, Finklea L, Zile MR, Spinale FG. Specific temporal profile of matrix metalloproteinase release occurs in patients after myocardial infarction: relation to left ventricular remodeling. Circulation 114: 1020–1027, 2006.

44. Wilson WR, Anderton M, Schwalbe EC, Jones JL, Furness PN, Bell PR, Thompson MM. Matrix metalloproteinase-8 and -9 are increased at the site of abdominal aortic aneurysm rupture. Circulation 113: 438–445, 2006.

45. Winer J, Jung CK, Shackel I, Williams PM. Development and validation of real-time quantitative reverse transcriptase-polymerase chain reaction for monitoring gene expression in cardiac myocytes in vitro. Anal Biochem 270: 41–49, 1999.

AUTONOMIC
NEUROSCIENCE:
Basic & Clinical

Regional difference in ischaemia-induced myocardial interstitial noradrenaline and acetylcholine releases

Toru Kawada [a,*], Toji Yamazaki [b], Tsuyoshi Akiyama [b], Toshiaki Shishido [a], Shuji Shimizu [a],
Masaki Mizuno [a], Hidezo Mori [b], Masaru Sugimachi [a]

[a] *Department of Cardiovascular Dynamics, Advanced Medical Engineering Center, National Cardiovascular Center Research Institute,*
5-7-1 Fujishirodai, Suita, Osaka 565-8565, Japan
[b] *Department of Cardiac Physiology, National Cardiovascular Center Research Institute, Japan*

Abstract

Knowledge of the regional differences in myocardial interstitial noradrenaline (NA) and acetylcholine (ACh) levels during ischaemia would be important to understand the abnormality of neuronal environment surrounding the ischaemic heart. Using a cardiac microdialysis technique, we compared ischaemia-induced changes in the myocardial interstitial NA and ACh levels among three groups of anesthetized cats: the anterior free wall of the left ventricle (ANT group, $n=7$; the left anterior descending coronary artery was occluded), the posterior free wall of the left ventricle (POST group, $n=6$; the left circumflex coronary artery was occluded), and the right ventricle (RV group, $n=6$; the right coronary artery was occluded). The maximum NA level was not different between the ANT and POST groups but was significantly lower in the RV group ($P<0.01$) [70 nM (SD 37), 106 nM (SD 99), and 7 nM (SD 10), respectively]. The maximum ACh level was not different between the ANT and POST groups but was significantly lower in the RV group ($P<0.05$) [16 nM (SD 7), 20 nM (SD 15), and 6 nM (SD 2), respectively]. In contrast, there were no significant differences in NA or ACh release in response to a local administration of ouabain (10 mM) among the ANT, POST, and RV groups ($n=6$ each). In conclusion, the regional difference of the ischaemic effects, rather than the regional difference in the functional distributions of sympathetic and vagal efferent nerve terminals, might contribute to the lower levels of ischaemia-induced NA and ACh releases in the RV group.

The heart is under an incessant control by the autonomic nervous system. The principal molecule that affects the myocardium is noradrenaline (NA) for the sympathetic nerve and acetylcholine (ACh) for the parasympathetic nerve. Acute myocardial ischaemia causes abnormality of the neural regulation via mechanisms such as pathological cardiocardiac reflexes and disruption of the nerves traversing the ischaemic region (Zipes 1990; Hainsworth, 1991; Elvan and Zipes, 1998; Armour, 1999; Kawada et al., 2002). Although occlusion of the left anterior descending coronary artery

(LAD) has been shown to increase myocardial interstitial NA and ACh levels in the ischaemic region (Shindo et al., 1996; Kawada et al., 2000; Lameris et al., 2000), whether the effects of ischaemia on the myocardial interstitial NA and ACh levels are homogeneous within the left ventricle and between the left and right ventricles remains unknown. The cardiodepressor reflex similar to that induced by veratridine (the Bezold–Jarisch reflex) is frequently observed in inferoposterior but not in anterior myocardial infarction, suggesting the regional difference in the vagal afferent fibre distribution within the left ventricle (Thames et al., 1978; Walker et al., 1978). Regional differences are also reported in the distributions of sympathetic and vagal efferent nerves within the left ventricle and between the left and right ventricles

* Corresponding author. Tel.: +81 6 6833 5012x2427; fax: +81 6 6835 5403.
E-mail address: torukawa@res.ncvc.go.jp (T. Kawada).

(Pierpont et al., 1984; Schmid et al., 1978). We hypothesized that the effects of ischaemia on the myocardial interstitial NA and ACh levels would also show regional differences.

We used a cardiac microdialysis technique and measured dialysate NA and ACh concentrations as indices of myocardial interstitial NA and ACh levels in anesthetized cats (Akiyama et al., 1991, 1994; Yamazaki et al., 1997; Kawada et al., 2001). We compared ischaemia-induced changes in the myocardial interstitial NA and ACh levels among the following regions: the anterior free wall of the left ventricle (ANT group) perfused by the LAD, the posterior free wall of the left ventricle (POST group) perfused by the left circumflex coronary artery (LCX), and the right ventricle (RV group) perfused by the right coronary artery (RCA). In addition, we compared changes in the myocardial interstitial NA and ACh levels in response to a local administration of ouabain through the dialysis probe (Yamazaki et al., 1999; Kawada et al., 2001). The advantage of the local administration of ouabain might be that we can assess the transmitter releasing function of the sympathetic and vagal efferent nerve terminals in the working heart without significant effects on the systemic haemodynamics.

1. Materials and methods

1.1. Surgical preparation

Animal care was conducted in accordance with the *Guiding Principles for the Care and Use of Animals in the Field of Physiological Sciences* approved by the Physiological Society of Japan. All protocols were approved by the Animal Subjects Committee of the National Cardiovascular Center. Adult cats weighing 2.2 to 5.0 kg were anaesthetized via an intraperitoneal injection of pentobarbital sodium (30–35 mg/kg) and ventilated mechanically with room air mixed with oxygen. The depth of anaesthesia was maintained with a continuous intravenous infusion of pentobarbital sodium $(1-2 \text{ mg kg}^{-1} \text{ h}^{-1})$ through a catheter inserted into the right femoral vein. Mean systemic arterial pressure was measured from a catheter inserted into the right femoral artery. The heart rate was determined using an electrocardiogram.

We performed an ischaemia protocol and a local ouabain protocol in different animals. In each protocol, the experimental animals were divided into ANT, POST, and RV groups. In the ANT and POST groups, the left fifth and/or sixth ribs were resected to allow access to the heart. In the ANT group, a 3-0 silk suture was passed around the LAD just distal to the first diagonal branch for later occlusion. Using a fine guiding needle, a dialysis probe was implanted transversely into the anterior free wall of the left ventricle perfused by the LAD. In the POST group, a 3-0 silk suture was passed around the LCX for later occlusion, and a dialysis probe was implanted transversely into the posterior free wall of the left ventricle perfused by the LCX. In the RV group, the right fifth and/or sixth ribs were resected to expose the heart. A 3-0 silk suture was passed around the RCA for later occlusion. The right ventricular wall was picked up with

a pair of forceps, and a dialysis probe was threaded transversely through the myocardium using a fine guiding needle. Heparin sodium (100 U/kg) was administered intravenously to prevent blood coagulation. A postmortem examination confirmed that the dialysis probe did not penetrate into the ventricular cavity. In the local ouabain protocol, similar experimental settings without a coronary snare were prepared for the three groups of animals.

1.2. Dialysis technique

The materials and properties of the dialysis probe have been described previously (Akiyama et al., 1991, 1994). Briefly, a dialysis fibre (13 mm length, 310 μm O.D., 200 μm I.D.; PAN-1200, 50,000 molecular weight cutoff, Asahi Chemical, Osaka, Japan) was glued at both ends to polyethylene tubes (25 cm length, 500 μm O.D., 200 μm I.D.). The dialysis probe was perfused at a rate of 2 μl/min with Ringer solution containing a cholinesterase inhibitor eserine (10^{-4} M). Two hours elapsed before the dialysate sampling was started to allow dialysate NA and ACh concentrations reached steady states. One sampling period was set at 15 min, which yielded a sample volume of 30 μl. The actual dialysate sampling lagged by 5 min behind a given collection period taking into account the dead space volume between the dialysis membrane and the sample tube. Each sample was collected in a microtube containing 3 μl of phosphate buffer
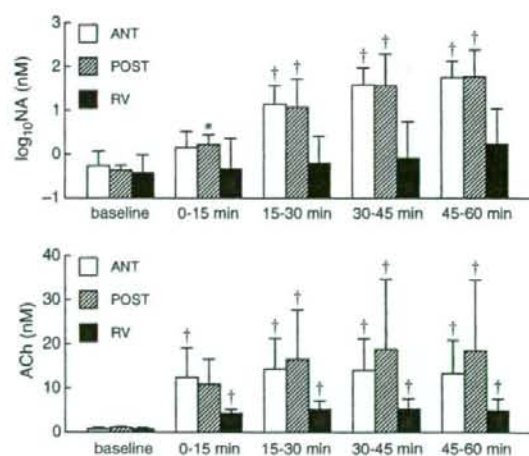

Fig. 1. Changes in myocardial interstitial noradrenaline (NA) and acetylcholine (ACh) levels during coronary occlusion. ANT: region of the anterior free wall of the left ventricle perfused by the left anterior descending coronary artery, POST: region of the posterior free wall of the left ventricle perfused by the left circumflex coronary artery, RV: region of the right ventricle perfused by the right coronary artery. The coronary occlusion significantly increased myocardial interstitial NA levels in the ANT and POST groups (top panel). Changes in the NA levels were not statistically significant in the RV group. The coronary occlusion significantly increased myocardial interstitial ACh levels in all of the ANT, POST, and RV groups (bottom panel). Data are mean and SD values. *$P<0.05$ and †$P<0.01$ from the corresponding baseline value by Dunnett's test.
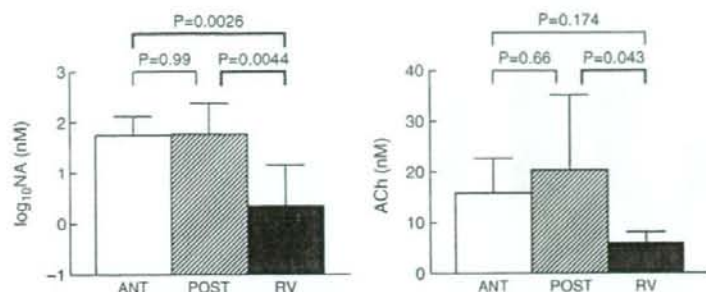
Fig. 2. Maximum levels of myocardial interstitial NA and ACh induced by coronary occlusions. The maximum NA level did not differ between the ANT and POST groups, but it was significantly lower in the RV group (left panel). The maximum ACh level did not differ between the ANT and POST groups, but it was significantly lower in the RV group than in the POST group (right panel). Data are mean and SD values. Exact P values determined by Tukey test are supplied.

(0.1 M, pH 3.5) to prevent amine oxidation. The ACh concentration in the dialysate was measured directly by high performance liquid chromatography with electrochemical detection (HPLC-ECD) system (Eicom, Kyoto, Japan). The NA concentration in the dialysate was measured by another HPLC-ECD system after removing interfering compounds with an alumina procedure.

1.3. Protocols

1.3.1. Ischaemia protocol

In each animal in the ANT ($n=7$), POST ($n=6$), and RV ($n=6$) groups, a 15-min dialysate sample was collected under baseline conditions. Thereafter, each corresponding coronary artery was occluded for 60 min, and four consecutive 15-min dialysate samples were obtained during the occlusion period.

1.3.2. Local ouabain protocol

In each animal in the ANT ($n=6$), POST ($n=6$), and RV ($n=6$) groups, a 15-min dialysate sample was collected under baseline conditions. The perfusate for the dialysis probe was then replaced with Ringer solution containing 10 mM of ouabain. The local administration of ouabain has been shown to evoke myocardial interstitial NA and ACh releases without significant effects on the systemic haemodynamics (Yamazaki et al., 1999; Kawada et al., 2001). Four consecutive 15-min dialysate samples were obtained during the local administration of ouabain.

1.4. Statistical analysis

All data are presented as mean (SD) values. Because the increase in NA reached more than 100 times the baseline value in the ANT and POST groups, NA data were compared after logarithmic transformation. To examine the effects of ischaemia or the local administration of ouabain on the NA or ACh level in each group, we used one-way repeated-measures analysis of variance (Glantz, 2002). When there was a significant difference in measured values among the collection periods, Dunnett's test was applied to identify the difference from the baseline value. To compare the maximum NA or ACh response among the ANT, POST, and RV groups, we used one-way analysis of variance. When there was a significant difference among the three groups, Tukey test was applied for simultaneous all pairwise comparisons. The differences were considered significant at $P<0.05$.

2. Results

Coronary artery occlusion increased the NA levels to more than 100 times the respective baseline levels in the ANT and POST groups (Fig. 1, top). In the RV group, although the mean NA level increased to nearly 10 times the baseline level, the change was not statistically significant, possibly due to the large variance of the NA responses across the animals. The coronary occlusion increased the ACh levels to approximately 15 times the respective baseline levels in the ANT and POST groups whereas it increased the

Table 1
Changes in mean arterial pressure by occlusions of the anterior descending coronary artery (ANT), the left circumflex coronary artery (POST), and the right coronary artery (RV)

	Baseline	5	15	30	45	60
ANT	116 (31)	114 (27)	108 (24)	108 (25)	108 (23)	110 (25)
POST	139 (31)	119 (31)†	125 (31)†	130 (31)*	132 (28)	135 (33)
RV	101 (20)	101 (26)	99 (22)	101 (23)	103 (25)	103 (23)

Baseline and values after 5, 15, 30, 45, and 60 min of the occlusion are presented (in mm Hg). Data are mean (SD) values. *$P<0.05$ and †$P<0.01$ from the corresponding baseline value.

Table 2
Changes in the heart rate by occlusions of the anterior descending coronary artery (ANT), the left circumflex coronary artery (POST), and the right coronary artery (RV)

	Baseline	5	15	30	45	60
ANT	193 (18)	166 (13)†	174 (15)†	175 (18)†	173 (15)†	171 (15)†
POST	183 (25)	159 (21)†	167 (20)†	167 (25)†	170 (25)†	169 (27)†
RV	188 (34)	175 (35)	176 (33)	179 (35)	181 (36)	183 (38)

Baseline and values after 5, 15, 30, 45, and 60 min of the occlusion are presented (in beats min^{-1}). Data are mean (SD) values. †$P<0.01$ from corresponding baseline value.
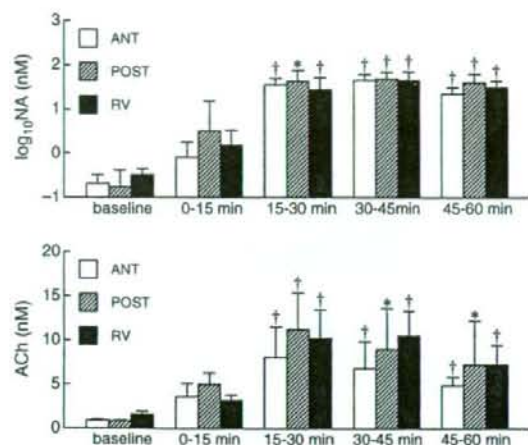
Fig. 3. Changes in myocardial interstitial NA and ACh levels induced by a local administration of ouabain through the dialysis probe. Ouabain significantly increased myocardial interstitial NA levels in all of the ANT, POST, and RV groups (top panel). The maximum NA level did not differ among the three groups. Ouabain significantly increased myocardial interstitial ACh levels in all of the ANT, POST, and RV groups (bottom panel). The maximum ACh level did not differ among the three groups. Data are mean and SD values. *$P<0.05$ and †$P<0.01$ from the corresponding baseline value by Dunnett's test.

ACh levels to approximately 8 times the baseline level in the RV group (Fig. 1, bottom).

The maximum NA level observed during ischaemia was not different between the ANT and POST groups, but it was significantly lower in the RV group than in the ANT and POST groups (Fig. 2, left). The maximum ACh level observed during ischaemia was not different between the ANT and POST groups, but it was significantly lower in the RV group than in the POST group (Fig. 2, right).

Changes in mean arterial pressure obtained from the ischaemia protocol are summarized in Table 1. Occlusion of the LAD did not change mean arterial pressure significantly (the ANT group), whereas occlusion of the LCX significantly decreased mean arterial pressure at 5, 15, and 30 min of the ischaemic period (the POST group). Occlusion of the RCA did not change mean arterial pressure (the RV group).

Changes in the heart rate obtained from the ischaemia protocol are summarized in Table 2. Occlusion of the LAD significantly decreased the heart rate throughout the occlusion period (the ANT group). Occlusion of the LCX also significantly decreased the heart rate throughout the occlusion period (the POST group). In contrast, occlusion of the RCA did not change the heart rate significantly (the RV group).

A local administration of ouabain increased the NA levels in all of the ANT, POST, and RV groups (Fig. 3, top). There were no significant differences in the maximum NA levels among the three groups ($P=0.40$ by ANOVA). The local administration of ouabain also increased the ACh levels in all of the ANT, POST, and RV groups (Fig. 3, bottom). The ACh levels reached their maximum levels during 15–30 min

of the administration period, then slightly decreased from the maximum levels during 30–45 and 45–60 min of the administration period but remained higher than the respective baseline levels. There were no significant differences in the maximum ACh levels among the three groups ($P=0.35$ by ANOVA).

3. Discussion

The level of ischaemia-induced NA release was significantly lower in the RV group than in the ANT and POST groups (Fig. 2, left). The level of ischaemia-induced ACh release was significantly lower in the RV group than in the POST group (Fig. 2, right). To our knowledge, this is the first report showing the differential effects of ischaemia on the myocardial interstitial NA and ACh levels among the main coronary arteries.

3.1. Regional difference in the ischaemia-induced myocardial interstitial NA release

Mechanisms responsible for the ischaemia-induced NA release have been extensively studied (Schömig A et al., 1984, 1988). An exocytotic release mechanism participates in the NA release in the early phase of ischaemia (within approximately 20 min from the onset of ischaemia) (Akiyama and Yamazaki, 1999). Energy depletion in the ischaemic region impairs the Na^+–K^+ ATPase activity and induces axoplasmic Na^+ accumulation. Because the NA uptake carrier is driven by the Na^+ gradient across the plasma membrane (Schwartz, 2000), the accumulation of intracellular Na^+ causes the reverse transport of axoplasmic NA to extracellular space. This nonexocytotic release mechanism becomes predominant as the ischaemic period is prolonged (Akiyama and Yamazaki, 1999; Lameris et al., 2000). In the present study, there was no significant difference in the levels of ischaemia-induced NA release between the ANT and POST groups (Fig. 2, left), suggesting that the extent of energy depletion caused by the coronary artery occlusion might be similar between the anterior and posterior regions of the left ventricle. In contrast, the level of ischaemia-induced NA release was much lower in the RV group (Fig. 2, left). Much lower oxygen consumption in the right ventricle than in the left ventricle (Weiss et al., 1978; Kusachi et al. 1982) may have delayed the progression of ischaemia and/or mitigated the severity of ischaemia.

To examine whether the observed difference in the ischaemia-induced NA release was attributable to the regional difference in the functional distribution of sympathetic efferent nerve terminals, we measured the amount of myocardial interstitial NA release in response to a local administration of ouabain (Yamazaki et al., 1999). Because locally administered ouabain spreads in the vicinity of the semipermeable membrane of the dialysis fibre and evokes the NA release, the NA concentration in the dialysate thus measured is considered to reflect the density of sympathetic

nerve terminals around the dialysis fibre. There were no significant differences in the maximum NA levels in response to the ouabain administration among the ANT, POST, and RV groups (Fig. 3, top), suggesting that the functional distribution of sympathetic efferent nerve terminals did not account for the lower level of ischaemia-induced NA release in the RV group.

The results of local administration of ouabain, showing no significant regional differences in the functional distribution of sympathetic efferent nerve terminals, are comparable to histological studies. In the human heart (Kawano et al., 2003), the number of tyrosine hydroxylase (TH)-positive nerves is similar between the left and right ventricles, and the number of TH-positive nerves in the anterior wall is 1.2 times greater than that in the posterior wall of the left ventricle. Although Pierpont et al. (Pierpont et al., 1984) reported a regional difference in the NA content in the canine left ventricle, the major difference observed in their study is an increasing gradient of NA from the apex to the base of the ventricle. In addition, the NA content was similar between the left and right ventricles in their study [495 ng/g (SD 267) vs. 503 ng/g (SD 123)].

3.2. Regional difference in the ischaemia-induced myocardial interstitial ACh release

In previous studies, we have demonstrated that acute myocardial ischaemia causes myocardial interstitial ACh release in the ischaemic region (Kawada et al., 2000; 2006b). An exocytotic release mechanism may be involved in the ischaemia-induced ACh release within approximately 15 min from the onset of ischaemia (Kawada et al., 2000, 2006a). Thereafter, a local ACh release mechanism independent of vagal nerve discharge may play a dominant role in the ischaemia-induced ACh release. In the present study, there was no significant difference in the levels of ischaemia-induced ACh release between the ANT and POST groups (Fig. 2, right). In contrast, the level of ischaemia-induced ACh release was much lower in the RV group than in the POST group. These results suggest that the energy depletion during ischaemia might be less severe or delayed in the right ventricle compared to that in the left ventricle.

Similar to the ouabain-induced NA release, there were no significant differences in the levels of ouabain-induced ACh release among the ANT, POST, and RV groups (Fig. 3, bottom). In a histological study of the human heart (Kawano et al., 2003), the number of acetylcholine esterase (AChE)-positive nerves in the right ventricle is 1.2 times greater than that in the left ventricle, and the number of AChE-positive nerves in the posterior wall is 1.4 times greater than that in the anterior wall of the left ventricle. In the guinea pig heart, the level of choline acetyltransferase activity was approximately two times higher in the right ventricle than in the left ventricle (Schmid et al., 1978). Notwithstanding the discrepancies among reports, these histochemical studies indicate that the number of the vagal nerve terminals in the right

ventricle is not less than that in the left ventricle. In other words, the regional difference in the vagal efferent nerve distribution may not account for the lower level of ischaemia-induced ACh release in the RV group as compared with the POST group.

3.3. Pathological significance

The pathological significance of the NA and ACh releases in the ischaemic region is still to be explored. Although high levels of NA reveal cardiotoxicity (Rona, 1985), depletion of catecholamine in reserpinized animals fails to reduce the myocardial infarct size (Toombs et al., 1993; Vander Heide et al., 1995). However, in the reserpinized animals, not only the ischaemic area but also the non-ischaemic area is subjected to catecholamine depletion, making the interpretation of the results difficult. Acetylcholine, when administered prior to coronary occlusion, induces an ischaemic preconditioning mimetic effect (Qin et al., 2002). Acetylcholine also exerts protection on myocytes against hypoxia (Kakinuma et al., 2005). Generally speaking, the excess NA might be harmful whereas the presence of ACh might be beneficial to the myocardium.

One possible feature of the cardiac microdialysis may be that it can monitor the time course of changes in myocardial interstitial NA and ACh levels (Shindo et al., 1996; Kawada et al., 2000; Lameris et al., 2000). Although myocardial ischaemia evokes both the NA and ACh releases, the ACh release is more prompt compared to the NA release. When calculating the percentage against the respective maximum level, the mean NA levels were only 3 and 2% whereas the mean ACh levels reached 79 and 53% in the ANT and POST groups, respectively, during the 0–15 min of the ischaemic period (Fig. 1, note the logarithmic scaling in the top panel). In the RV group, the mean NA level was 28% whereas the mean ACh level reached 72% during the 0–15 min of the ischaemic period. It seems that the ACh release is a protective mechanism against a forthcoming excess of NA in the ischaemic region. Further studies are required to elucidate the significance of a local neuronal environment in modifying the severity of myocardial ischaemia.

3.4. Regional difference in the reflex effects

In the ischaemia protocol, the reflexes from the heart and the arterial baroreflex might have modified the efferent nerve activities. Both the ANT and POST groups showed a significant decrease in the heart rate during ischaemia (Table 2), suggesting an increase in the vagal tone and/or a decrease in the sympathetic tone. Because mean arterial pressure was either unchanged (the ANT group) or decreased (the POST group) (Table 1), the baroreflex cannot account for the decrease in the heart rate during ischaemia. The decreased mean arterial pressure in the POST group compared to the unchanged mean arterial pressure in the ANT group suggests that the cardiodepressor reflex was stronger in the POST than

the ANT group. These differences, however, did not cause the difference in the maximum levels of ischaemia-induced NA and ACh releases between the ANT and POST groups (Fig. 2). Because local release mechanisms became predominant as the ischaemic period is prolonged (Akiyama and Yamazaki, 1999; Kawada et al., 2000, 2006a; Lameris et al., 2000), the difference in the efferent nerve activities might not have affected the maximum levels of NA and ACh releases significantly. In contrast to the ANT and POST groups, the RV group did not show significant changes in mean arterial pressure or the heart rate, suggesting that the effect of RCA occlusion on the systemic haemodynamics was minimal in the present study. Despite the absence of significant bradycardia, the myocardial interstitial ACh level was significantly increased in the RV group during ischaemia, suggesting the involvement of a local release mechanism.

There are limitations to the present study. First, we could not examine regional differences in the NA and ACh releases along the transmural axis from the epicardial layer to the endocardial layer, because we could not control the exact depth of the dialysis fibre implanted transversely in the ventricular wall. Second, species differences should be taken into account when interpreting the present data. As an example, we usually observed a bradycardic response not only during LCX occlusion but also during LAD occlusion in cats (Table 2). In contrast, LAD occlusion in dogs more frequently evokes tachycardia and hypertension (Thames et al., 1978; Zipes, 1990).

4. Conclusion

The maximum levels of ischaemia-induced NA and ACh releases did not differ between the ANT and POST groups but were significantly lower in the RV group. In contrast, myocardial interstitial NA and ACh releases in response to a local administration of ouabain did not show regional differences among the ANT, POST, and RV groups. The regional difference in the ischaemic effects, rather than the regional difference in the functional distributions of sympathetic and vagal efferent nerve terminals, might contribute to the lower levels of ischaemia-induced NA and ACh releases in the RV group.

Acknowledgments

References

Akiyama, T., Yamazaki, T., 1999. Norepinephrine release from cardiac sympathetic nerve endings in the in vivo ischemic region. J. Cardiovasc. Pharmacol. 34, S11–S14.

Akiyama, T., Yamazaki, T., Ninomiya, I., 1991. In vivo monitoring of myocardial interstitial norepinephrine by dialysis technique. Am. J. Physiol, Heart Circ. Physiol. 261, H1643–H1647.

Akiyama, T., Yamazaki, T., Ninomiya, I., 1994. In vivo detection of endogenous acetylcholine release in cat ventricles. Am. J. Physiol, Heart Circ. Physiol. 266, H854–H860.

Armour, J.A., 1999. Myocardial ischaemia and the cardiac nervous system. Cardiovasc. Res. 41, 41–54.

Elvan, A., Zipes, D.P., 1998. Right ventricular infarction causes heterogeneous autonomic denervation of the viable peri-infarct area. Circulation 97, 484–492.

Glantz, S.A., 2002. Primer of Biostatistics, 5th ed. McGraw-Hill, New York.

Hainsworth, R., 1991. Reflexes from the heart. Physiol. Rev. 71, 617–658.

Kakinuma, Y., Ando, M., Kuwabara, M., Katare, R.G., Okudela, K., Kobayashi, M., Sato, T., 2005. Acetylcholine from vagal stimulation protects cardiomyocytes against ischemia and hypoxia involving additive non-hypoxic induction of HIF-1alpha. FEBS Lett. 579, 2111–2118.

Kawada, T., Yamazaki, T., Akiyama, T., Sato, T., Shishido, T., Inagaki, M., Takaki, M., Sugimachi, M., Sunagawa, K., 2000. Differential acetylcholine release mechanisms in the ischemic and non-ischemic myocardium. J. Mol. Cell Cardiol. 32, 405–414.

Kawada, T., Yamazaki, T., Akiyama, T., Shishido, T., Inagaki, M., Uemura, K., Miyamoto, T., Sugimachi, M., Takaki, H., Sunagawa, K., 2001. In vivo assessment of acetylcholine-releasing function at cardiac vagal nerve terminals. Am. J. Physiol, Heart Circ. Physiol. 281, H139–H145.

Kawada, T., Yamazaki, T., Akiyama, T., Mori, H., Uemura, K., Miyamoto, T., Sugimachi, M., Sunagawa, K., 2002. Disruption of vagal efferent axon and nerve terminal function in the postischemic myocardium. Am. J. Physiol, Heart Circ. Physiol. 283, H2687–H2691.

Kawada, T., Yamazaki, T., Akiyama, T., Li, M., Ariumi, H., Mori, H., Sunagawa, K., Sugimachi, M., 2006a. Vagal stimulation suppresses ischemia-induced myocardial interstitial norepinephrine release. Life Sci. 78, 882–887.

Kawada, T., Yamazaki, T., Akiyama, T., Uemura, K., Kamiya, A., Shishido, T., Mori, H., Sugimachi, M., 2006b. Effects of Ca^{2+} channel antagonists on nerve stimulation-induced and ischemia-induced myocardial interstitial acetylcholine release in cats. Am. J. Physiol, Heart Circ. Physiol. 291, H2187–H2191.

Kawano, H., Okada, R., Yano, K., 2003. Histological study on the distribution of autonomic nerves in the human heart. Heart Vessels 18, 32–39.

Kusachi, S., Nishiyama, O., Yasuhara, K., Saito, D., Haraoka, S., Nagashima, H., 1982. Right and left ventricular oxygen metabolism in open-chest dogs. Am. J. Physiol, Heart Circ. Physiol. 243, H761–H766.

Lameris, T.W., de Zeeuw, S., Alberts, G., Boomsma, F., Duncker, D.J., Verdouw, P.D., Veld, A.J., van Den Meiracker, A.H., 2000. Time course and mechanism of myocardial catecholamine release during transient ischemia in vivo. Circulation 101, 2645–2650.

Pierpont, G.L., DeMaster, E.G., Cohn, J.N., 1984. Regional differences in adrenergic function within the left ventricle. Am. J. Physiol, Heart Circ. Physiol. 246, H824–H829.

Qin, Q., Downey, J.M., Cohen, M.V., 2002. Acetylcholine but not adenosine triggers preconditioning through PI3-kinase and a tyrosine kinase. Am. J. Physiol, Heart Circ. Physiol. 284, H727–H734.

Rona, G., 1985. Catecholamine cardiotoxicity. J. Mol. Cell Cardiol. 17, 291–306.

Schömig, A., Dart, A.M., Dietz, R., Mayer, E., Kübler, W., 1984. Release of endogenous catecholamines in the ischemic myocardium of the rat Part. A: locally mediated release. Circ. Res. 55, 689–701.

Schömig, A., Kurz, T., Richardt, G., Schömig, E., 1988. Neuronal sodium homeostasis and axoplasmic amine concentration determine calcium-independent noradrenaline release in normoxic and ischemic rat heart. Circ. Res. 63, 214–226.

Schmid, P.G., Greif, B.J., Lund, D.D., Roskoski Jr., R., 1978. Regional choline acetyltransferase activity in the guinea pig heart. Circ. Res. 42, 657–660.

Schwartz, J.H., 2000. Neurotransmitters. In: Kandel, E.R., Schwartz, J.H., Jessell, T.M. (Eds.), Principles of Neural Science, 4th ed. McGraw-Hill, New York, pp. 280–297.

Shindo, T., Akiyama, T., Yamazaki, T., Ninomiya, I., 1996. Regional myocardial interstitial norepinephrine kinetics during coronary occlusion and reperfusion. Am. J. Physiol, Heart Circ. Physiol. 270, H245–H251.

Thames, M.D., Klopfenstein, H.S., Abboud, F.M., Mark, A.L., Walker, J.L., 1978. Preferential distribution of inhibitory cardiac receptors with vagal afferents to the inferoposterior wall of the left ventricle activated during coronary occlusion in the dog. Circ. Res. 43, 512–519.

Toombs, C.F., Wiltse, A.L., Shebuski, R.J., 1993. Ischemic preconditioning fails to limit infarct size in reserpinized rabbit myocardium. Implication of norepinephrine release in the preconditioning effect. Circulation 88, 2351–2358.

Vander Heide, R.S., Schwartz, L.M., Jennings, R.B., Reimer, K.A., 1995. Effect of catecholamine depletion on myocardial infarct size in dogs: role of catecholamines in ischemic preconditioning. Cardiovasc. Res. 30, 656–662.

Walker, J.L., Thames, M.D., Abboud, F.M., Mark, A.L., Klopfenstein, H.S., 1978. Preferential distribution of inhibitory cardiac receptors in left ventricle of the dog. Am. J. Physiol, Heart Circ. Physiol. 235, H188–H192.

Weiss, H.R., Neubauer, J.A., Lipp, J.A., Shinha, A.K., 1978. Quantitative determination of regional oxygen consumption in the dog heart. Circ. Res. 42, 394–401.

Yamazaki, T., Akiyama, T., Kitagawa, H., Takauchi, Y., Kawada, T., Sunagawa, K., 1997. A new, concise dialysis approach to assessment of cardiac sympathetic nerve terminal abnormalities. Am. J. Physiol, Heart Circ. Physiol. 272, H1182–H1187.

Yamazaki, T., Akiyama, T., Kawada, T., 1999. Effects of ouabain on in situ cardiac sympathetic nerve endings. Neurochem. Int. 35, 439–445.

Zipes, D.P., 1990. Influence of myocardial ischemia and infarction on autonomic innervation of heart. Circulation 82, 1095–1105.

Angiotensin II attenuates myocardial interstitial acetylcholine release in response to vagal stimulation

Toru Kawada,[1] Toji Yamazaki,[2] Tsuyoshi Akiyama,[2] Meihua Li,[1,3] Can Zheng,[1,3] Toshiaki Shishido,[1] Hidezo Mori,[2] and Masaru Sugimachi[1]

[1]*Department of Cardiovascular Dynamics, Advanced Medical Engineering Center and* [2]*Department of Cardiac Physiology, National Cardiovascular Center Research Institute, Osaka; and* [3]*Japan Association for the Advancement of Medical Equipment, Tokyo, Japan*

Kawada T, Yamazaki T, Akiyama T, Li M, Zheng C, Shishido T, Mori H, Sugimachi M. Angiotensin II attenuates myocardial interstitial acetylcholine release in response to vagal stimulation. *Am J Physiol Heart Circ Physiol* 293: H2516–H2522, 2007. First published July 20, 2007; doi:10.1152/ajpheart.00424.2007.—Although ANG II exerts a variety of effects on the cardiovascular system, its effects on the peripheral parasympathetic neurotransmission have only been evaluated by changes in heart rate (an effect on the sinus node). To elucidate the effect of ANG II on the parasympathetic neurotransmission in the left ventricle, we measured myocardial interstitial ACh release in response to vagal stimulation (1 ms, 10 V, 20 Hz) using cardiac microdialysis in anesthetized cats. In a control group ($n = 6$), vagal stimulation increased the ACh level from 0.85 ± 0.03 to 10.7 ± 1.0 (SE) nM. Intravenous administration of ANG II at 10 $\mu g \cdot kg^{-1} \cdot h^{-1}$ suppressed the stimulation-induced ACh release to 7.5 ± 0.6 nM ($P < 0.01$). In a group with pretreatment of intravenous ANG II receptor subtype 1 (AT_1 receptor) blocker losartan (10 mg/kg, $n = 6$), ANG II was unable to inhibit the stimulation-induced ACh release (8.6 ± 1.5 vs. 8.4 ± 1.7 nM). In contrast, in a group with local administration of losartan (10 mM, $n = 6$) through the dialysis probe, ANG II inhibited the stimulation-induced ACh release (8.0 ± 0.8 vs. 5.8 ± 1.0 nM, $P < 0.05$). In conclusion, intravenous ANG II significantly inhibited the parasympathetic neurotransmission through AT_1 receptors. The failure of local losartan administration to nullify the inhibitory effect of ANG II on the stimulation-induced ACh release indicates that the site of this inhibitory action is likely at parasympathetic ganglia rather than at postganglionic vagal nerve terminals.

cardiac microdialysis; cats; losartan

ANG II HAS a variety of effects on the cardiovascular system (22): it acts on the vascular beds to increase peripheral vascular resistance and also on the adrenal cortex to cause volume retention. These direct effects of ANG II contribute to the maintenance of arterial pressure (AP). Aside from these direct effects, ANG II has been shown to modulate the sympathetic nervous system both centrally (7, 9) and peripherally (10). With respect to the sympathetic regulation in the heart, however, exogenous ANG II does not facilitate stimulation- and ischemia-induced norepinephrine release in the porcine left ventricle (18). Compared with a number of reports on the sympathetic system, only a few reports are available as to the effects of ANG II on the parasympathetic system. In 1982, Potter (23) demonstrated that ANG II (5–10 μg iv, body wt not

reported) inhibited bradycardia induced by vagal stimulation in dogs. In that study, administration of ACh reduced the heart rate to an identical degree in the presence or absence of ANG II, suggesting that the inhibition of bradycardia by ANG II was attributable to the inhibition of the ACh release from the vagal nerve terminals. In contrast, Andrews et al. (3) reported that ANG II (500 ng/kg iv) did not inhibit bradycardia induced by vagal stimulation in ferrets. In a rat heart failure model, ANG II receptor subtype 1 (AT_1 receptor) antagonist losartan enhanced the bradycardic response to vagal stimulation (5). In pithed rats, an angiotensin-converting enzyme (ACE) inhibitor captopril also enhanced the bradycardic response to vagal stimulation (25, 26). In all of these studies, changes in the heart rate were used as a functional measurement of peripheral vagal function because of the difficulty in measuring the ACh release in the in vivo heart. Accordingly, whether ANG II affects the vagal control over the ventricle remains unknown. The aim of the present study was to examine the effect of ANG II on the vagal stimulation-induced ACh release in the left ventricular myocardium by measuring the interstitial ACh levels directly using a cardiac microdialysis technique (1, 13–15). We also explored the possible sites of action for the effect of ANG II on the stimulation-induced ACh release by administering losartan systemically from the femoral vein or locally through the dialysis fiber. Because ACh has a protective effect on the ischemic myocardium (12, 24, 29), elucidating the effect of ANG II on the ACh release in the ventricle would be helpful to understand the mechanism of ACE inhibitor or AT_1 receptor antagonist for the treatment of heart diseases (16, 17).

MATERIALS AND METHODS

Surgical Preparation

Animal care was provided in strict accordance with the *Guiding Principles for the Care and Use of Animals in the Field of Physiological Sciences* approved by the Physiological Society of Japan. All protocols were approved by the Animal Subject Committee of the National Cardiovascular Center. Twenty eight adult cats weighing from 1.9 to 4.9 kg were anesthetized using an intraperitoneal injection of pentobarbital sodium (30–35 mg/kg) and were then ventilated mechanically with room air mixed with oxygen. The depth of anesthesia was maintained by a continuous intravenous infusion of pentobarbital sodium ($1–2$ mg $\cdot kg^{-1} \cdot h^{-1}$) through a catheter inserted in the right femoral vein. Systemic AP was monitored by a catheter inserted in the right femoral artery. Heart rate was determined from an